Counting Algorithm of Microorganism and Control of Bioreactor System

미생물의 계수 알고리즘과 생물반응기 시스템의 제어

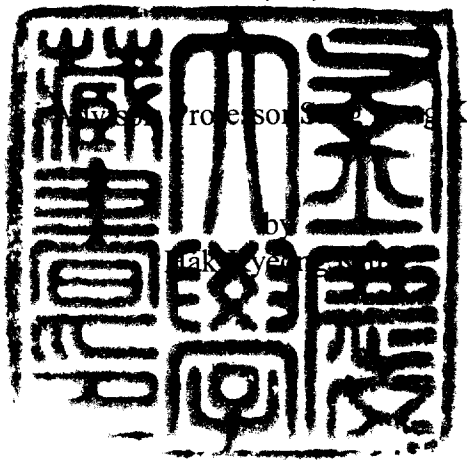

by

[illegible]

A thesis submitted in partial fulfillment of the requirements for the degree of

Doctor of Philosophy

In the Department of Mechatronics Engineering, Graduate School, Pukyong National University

February 2002

Counting Algorithm of Microorganism and Control of Bioreactor System

A Dissertation
by

Hak-Kyeong Kim

Approved as to style and content by:

Gi Sik Byun
Chairman

Dean of Graduate School

Hwan Seong Kim
Member

Myung Suk Lee
Member

Sang Bong Kim
Member

Tan Tien Nguyen
Member

February 2002

Contents

Counting Algorithm of Microorganism and Control of Bioreactor System

Hak-Kyeong Kim

Department of Mechatronics Engineering
Graduate School
PUKYONG National University

Abstract

This thesis proposes the counting algorithms of microorganism in bioreactor and the design method of theoretical control system for controlling bioreactor system. The counting at each growing steps of microorganism is very important in order to control bioreactor system. There are a viable cell counting method using culture medium of microorganism and a direct counting method using a microscope in traditional methods for counting microorganism. A viable cell counting method has small errors. But it is too time-consuming for counting microorganisms due to cultivating them over 24 hours. A direct counting method using a microscope has large error because microorganisms are directly counted by human visual method. In case of controlling bioreactor system in a real time, a fast and precise counting method is needed since the direct counting of microorganisms by human visual method cannot be used. In case of using digital

image processing method, microscopic images are obtained by interface circuit for electrical signal processing and CCD camera on microscope. So the microscopic images include a lot of noises, un-uniform gray value and overlapped images, etc. This makes the precise counting of microorganisms be difficult. To solve this problem, this thesis proposes the counting algorithms of microorganism with the process removing the several types of noises and eliminating un-uniform gray values of background from initial microscopic image obtained by CCD camera. For the elimination of noises and the uniformity of background, this thesis uses morphological filters and minimum error method, two dimensional cubic surface fitting method and bilinear interpolation.

This thesis also proposes the counting algorithm of microorganism in filtered images. This is a new algorithm hybridizing Otsu's automatic optimal thresholding method, traditional watershed algorithm and elongating marker algorithm. The Otsu's method decides the optimal thresholding value automatically. The proposed elongating marker algorithm improves the imprecise counting by preventing over-segmentation of overlapped images produced by the traditional watershed algorithm. The effectiveness of the proposed methods is shown through the results applying Otsu's method, human visual method and conventional watershed algorithm to yeast and ammonia-oxidizing bacteria.

As the fundamental study to control microorganisms in bioreactor using the above proposed counting algorithms, this thesis proposes a nonlinear adaptive controller design method applicable to the process with non-linearity and a high gain observer design method for estimating system parameters and state variables. Nonlinear adaptive controller design method is proposed using backstepping method based on process model. It is shown that the controller design method can track the reference substrate concentration by regulating dilution rate even in the step change of reference substrate concentrate and influent concentration. The effectiveness of the proposed controller design method is shown though simulation results. As the result, it is shown that the proposed controller design

method can keep the substrate concentration constantly and smoothly increase biomass concentration by constantly increasing dilution rate even in the step change of reference substrate concentrate and influent concentration. The proposed observer design method is modified based on Busawon's high gain observer for estimating parameters and state variables of bioreactor system. The proposed observer uses an appropriate unbound and time-dependent function. The simulation results show that the estimation values using the proposed observer converges faster to their real values than using the well-known Busawon's observer.

I

Introduction

1.1 Background and Motivation

Counting and control for cultivating microorganism in bioreactor are very important.

Digital image processing method is used for counting microorganism. Today, digital image processing method plays an important role in many fields such as microbiology, electronics, etc. Image processing technique was firstly needed in areas of celestial physics and medical science. It was applied to geographic probing by satellite, MRI, CT image processing, automatic forged note detecting device and automatic lock system by character pattern recognition, fingerprint and face recognition using image processing method. Recently, image processing technique is using widely due to necessity of non-touching type of sensors for automation and information visualization using multimedia.

Specially, after microscopic image is obtained from CCD camera on microscope, image processing method is used to extract cell information in the microscopic image at the field of microbiology. But because microscopic images obtained from microscope have a lot of noises, it is not easy to segment object cells from images with noises. So thresholding value is important to remove the noises and segment object cells from images. There are histogram-based threshoding method, entropy-based threshoding method, fuzzy-based thresholding method and region-based thresholding method for the determination of thesholding value. There are Otsu's method[6], iterative method[68], Thrussel [69]

and minimum error method[71] for Histogram-based thesholding method. There are Kapur's method[55] and Pun's method[72] for entropy-base method. There are Fuzzy method and Yager method[70] for Fuzzy-based thresholding method. There are Chow and Kaneko method[73] for region-based method. Among the above methods, Otsu's method is used widely and generally. However, it is very difficult to remove noises of microscopic images and exactly count microbial cells on the images by only Otsu's method.

For example, at aquaculture plant with recirculation filtering system, because ammonia generated aggravates the quality of water and is harmful for fish life, the productivity of fish can be enhanced by elongating fish life using ammonia-oxidizing bacteria removing ammonia. It is necessary to count and control viable ammonia-oxidizing bacteria to manage aquaculture plant using ammonia-oxidizing bacteria. There are colony method and dilution method for viable cell counting method. Human visual method and microscopic method are largely in both counting method for the measurement of counting bacteria. A human visual counting method takes a long time to count microbial cell, while a microscopic counting method is used for counting microbial cell fast. The digital image processing method in a microscopic counting method is used to count microbial cell in a real time and with simplicity[15-17]. However, because the microbial cells are colorless and transparent, microbial cells must be dyed such as Syto 13, DAPI, etc. But because these dyes not only becomes faded very fast within 2~3 seconds and the dye degree of each cell is different but also background image has different gradient, it is difficult to apply the uniform thresholding value over the entire image. Furthermore, because binary image has a lot of overlapped image, the microbial cells counting methods by general segmentation method have limit to count the microbial cells exactly. So, it is necessary to develop an algorithm that can count microbial cells exactly under the condition of overlapped shape, the variation of thresholding value and various gradients of microscopic image according to the image positions.

Fermentation process is so complex, time varying and highly nonlinear. Due to cultivating methods, pH, dissolved oxygen, temperature, antifoam addition, biomass accumulation, production formation and nutrient depletion during fermentation process, the dynamic behavior is significantly changed. So it is difficult to make a model and control for fermentation process exactly. There are several control methods applied to bioreactor system below.

L. Chen, et al.[32] proposed general adaptive nonlinear method for the ethanol regulation in yeast production process by manipulating dilution rate in fed-batch biological bioreactors when ethanol concentration, dissolved oxygen concentration, CO2 concentration and gas outflow rate are measured online with fixed known influent substrate concentration, and unknown specific growth rate. M. Maher, et al.[33] developed adaptive filtering and estimation algorithms using extended Kalman filter, the Dochain-Bastin method and Zeng-Dahou method in a nonlinear fermentation process. G. Roux, et al.[30] proposed adaptive nonlinear method by using an operation of projection for controlling alcoholic fermentation process in continuous stirred tank bioreactor. The good regulation profiles and tracking the temporal evaluation of certain biological parameters were presented by their proposed method. R. Schneider, et al[31] proposed adaptive model-based prediction control to control the state variables of the process around a defined trajectory for the fed-batch fermentation process. Sliding-mode method for controlling fermentation process has been applied for tracking reference substrate concentration by using dilution rate as control variable [25-27]. Miroslav Krstic[29] applied adaptive back-stepping method for control of biochemical process with assuming of constant dilution rate and defined specific growth rate function. This function includes two unknown parameters. Yet there is no way of deriving such function from the known models of specific growth rate. It is necessary to keep constant substrate concentration in bioreactor. So to track reference substrate concentration exactly, parameters and state variables for fermentation process in bioreactor must be known. However, it is impossible to

know these parameters and state variables because of non-linearity of fermentation process in bioreactor. So new algorithm is needed to track reference substrate exactly even though fermentation process is nonlinear in bioreactor.

On the other hand, it is difficult to make a model and control for fermentation process exactly. Specially, the exact estimate of the specific growth rate is so uncertain because it depends on parameters such as biomass concentration, substrate concentration, production formulation and temperature, etc. Despite the intensive effort spent in developing new biological sensors in recent years, the sensors are not much exact. To overcome these problems, observers, software sensors, for on-line monitoring biological variables has been developed.

The observer is expected to produce the estimate of the state of the original system. One of the reasons of using observer is that full state measurement of a process is generally not available. The construction of observers is very interesting and there are some available methods have been introduced in literatures. For a linear system, a standard solution is given by the classical Lubenburger observer. For a nonlinear system, the list of references at the end of the paper cover part of recent works done in the area. Gauthier et al.[82] proposed a simple observer for nonlinear system application to bioreactor under general technological assumptions. Farza et al.[79] proposed simple nonlinear observer for estimation in fermentation process. Martinez-Guerra et al.[75] proposed parametric and state estimation using high-gain nonlinear observers applied to bioreactor. Olivera et al.[80] solved the tuning problem of an observer-based algorithm for the on-line estimation of reaction rates in stirred tank bioreactors. Tonambe[83] reduced the estimation of the unknown parameters of a nonlinear system to the estimation of its state variables by a state space immersion using asymptotic high-gain observers. Busawon et al.[76-78] proposed simple high gain observer for a class of nonlinear systems in a special canonical observable form for state and parameter estimation in bioreactor. Among the above papers, the Busawon's high gain observer attained good performance and agreed well with

the experimental results. However in some cases, the estimated state of the system is not converged to its real value as fast as required.

1.2 Outline and Summary of Contributions

This paper has two objectives. One is to develop new algorithm to remove noises and count object cells in microscopic image obtained from CCD camera using digital image processing method. Another is to develop a new algorithm for cultivating process in bioreactor.

This paper consists of 6 chapters.

Chapter I is an introduction. Traditional methods and current methods are introduced for image processing method and controlling cultivating process. Background and research contents of this paper are introduced. Bioreactor system and the procedure that the image is obtained are introduced.

Chapter II proposed the method for extracting feature vectors that express morphological characteristics of microbial cells using image processing method. The effectiveness of the proposed method is shown by the results applied to yeast, *Zygosaccharomyces rouxii*.

Chapter III proposes elimination and reconstruction method of a background using minimum square error method, two dimensional 3rd order surface fitting and bilinear interpolation. The effectiveness of the propose method in the noise removal and segmentation of object cells from background is shown through the results applied to yeast, *Zygosaccharomyces rouxii* and ammonia-oxidizing bacteria, *Acinetobacter* sp.

Chapter IV proposes the method that hybridize traditional Otsu's method block, and the algorithm that elongates markers obtained by traditional watershed algorithm with 2×2 block processing to segment and count microbial cells on microscopic image. The results counted by the proposed method humane visual

method, traditional Otsu's method and traditional watershed algorithm are compared through the results applied to *Acinetobacter* sp.

Chapter V proposes nonlinear adaptive method for controlling cultivating process in bioreactor using backstepping method. Controller using backstepping method is designed to track reference substrate concentration and by regulating dilution rate even in the step change of reference substrate concentration and influent substrate concentration. The effectiveness of the proposed method is shown by the results of simulations.

Chapter VI proposed nonlinear observer for applications fermentation process in bioreactor. The proposed observer based on Busawon's high gain observer is modified by using a bounded appropriated time dependent function. It is applied to estimate the states in bioreactor. The effectiveness of the proposed observer is shown through simulation results.

Chapter VII summarizes the results of this paper.

1.3 Bioreactor System

A general bioreactor system structure is shown in Fig. 1. The bioreactor system is composed of air supply system, cooling and heating system, fermenting system, measurement system and control system. Air supply system consists of compressor, air tank, air flow meter, air valve and tubes for air-in and air-out. Cooling system is composed of valves, tubes for water-in and water-out and thermometer. Heating system consists of heater. Fermenting system consists of bioreactor, base and acid supply system controlled by peristaltic pump respectively for controlling pH and condensing system for separating vapour and condensed water. Base and acid supply system consists of pH meter, peristaltic pump and tube for supplying base and acid. Condensing system consists of condenser, valves and tubes for water-in and water-out and gas-out tube.

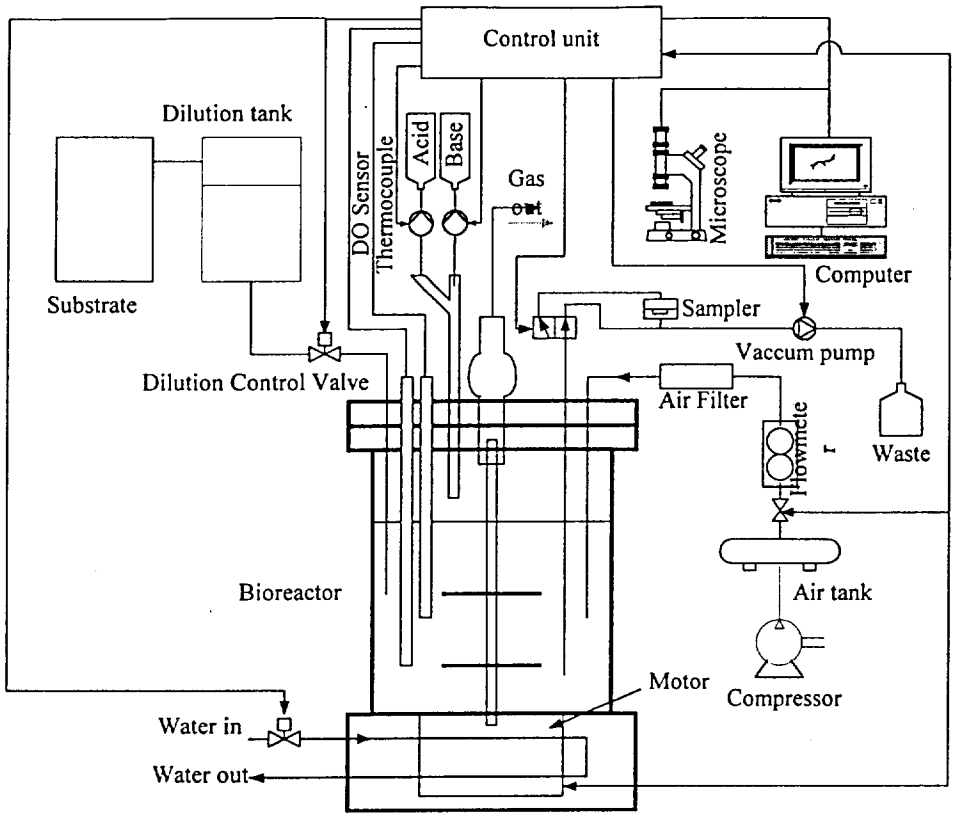

Fig. 1 Bioreactor system

Sensors consists of pH meter for measuring, pH in bioreactor, anti-form meter for measuring generated form, thermometer for measuring temperature in bioreactor, DO sensor, OD(optical density) system, motor velocity meter for measuring rotation velocity of the stirrer, flowmeter for measuring supply air rate. DO sensor is set to measure DO(dissolved oxygen) in the bioreactor after dipping it into O_2 zero gel and compensating it into 0(zero) ppm. OD system is used for measuring biomass of microorganisms in bioreactor. A solution of 0.1 $m\ell$ microorganisms is inoculated into the bioreactor. Sampling system consists of vacuum pump, filtering devices, nuclepore filter, tube, waste bottle and flowmeter for sampling flowrate. Dilution system is used to dilute sampled material. It consists of tube, tank, flowmeter and valve. Medium without microorganisms or tap water is used

for diluting sampled material. Dye is injected into filtering devices to dye microorganisms by using injection needle. Specimens consist of nuclepore filter with sampled microorganisms, cover glass and slide glass. Image processing system consists of microscope, CCD camera, frame grabber card and personal computer. The object is set up on the guide plate of the microscope and it is captured by CCD camera attached at the microscope and the captured image is changed into digital image by frame grabber interface card and the image sequence is analyzed by the developed image processing program package.

II

Morphological Feature Extraction of Microorganisms Using Image Processing

2.1 Introduction

Vision system, nowadays, has been widespread technology in several engineering fields since the relevant efforts appeared around 1964 at the J.P.L.(Jet Propulsion Laboratory) and concerned the digital process satellite images coming from the moon[7]. In cell technology, recent methods of digital image analysis include location and enumeration of bacteria in solid foods, *in situ* microscopy and image analysis for on-line monitoring of yeast fermentations[9], and texture analysis of fungal colonies for subsequent transfer. Notable recent applications include studies on the pulsatile growth of hyphal apices, biochemical differentiation of fungal colonies, and simple structural differentiation of mycelia from submerged fungal cultures [8].

All microscopic images have many obstacles on the lens and are directly affected by brightness of light source, staining method for cells, and settings of optical filters, etc. The microscopic image often has several special properties such as non-symmetric contour, a bimodal histogram, and multi-layer objects, etc. Non-symmetric contour is due to light source of the microscope concentrated on the center of the image. Luminance at the center of the background is higher than that of its surrounding. This property affects a gray-level histogram of the image

and makes the exact image segmentation difficult. Otsu's optimal threshold detection method is usually used for the image segmentation[6]. But the segmented image by only the Otsu's method includes a lot of noises. So extracting the exact feature vector from the image segmented by only Otsu's method is very difficult.

So this paper shows basic research results to develop vision analysis system that can be applied for bioprocess plant and to present a procedure extracting features in order to identify the object cells exactly under background with noise such as obstacles and non-symmetric contour, etc. The classification of object type is based on feature vector such as area, complexity, centroid, rotation angle, effective diameter, perimeter, width and height of the object. So the feature vector plays very important role in classifying objects. Because feature vector is affected by noises and holes, it is necessary to remove noises contaminated in original image to get the feature vector extraction exactly. In this paper, we propose the following method to do so. It presents a procedure that extracts features for vision analysis based on pattern recognition. The procedure works semi-automatically: operator has to find target organisms and adjust focus to get a clean picture manually, and next all following steps work full-automatically. First, several filters are applied to original images in order to clean them. Next, Otsu's optimal threshold selection method and morphological filters such as cleaning, filling and opening filters are employed to separate objects from background and to get rid of isolated particles respectively. The labeling step segments each objects by 4-adjacent neighborhood. The previous labeled image is filtered by area filter. Finally, from this area-filtered image, morphological features such as area, perimeter, complexity, centroid, rotation angle, width, height and effective diameter are extracted by the proposed procedure. To prove the effectiveness, the proposed method is applied for yeast *Zygosaccharomyces rouxii*. It is also shown that the experimental results from the proposed method is more efficient in

measuring feature vectors than from only Otsu's optimal threshold detection method.

2.2 Characteristics and Problem Statements of Microscopic Images

All microscopic images have many obstacles on the lens as shown in Fig. 2. They are directly affected by brightness of light source, staining method for cells, and settings of optical filters, etc. Understandings for microscopic image need to adopt the proper methods among a number of image processing techniques. Digital image is a kind of spatial frequency as shown in Fig. 3 that illustrates the relationship between brightness and gray values of image.

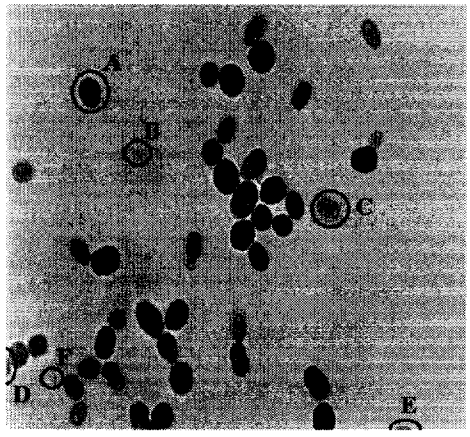

Fig. 2 Microscopic image of *Zygosaccharomyces rouxii.*

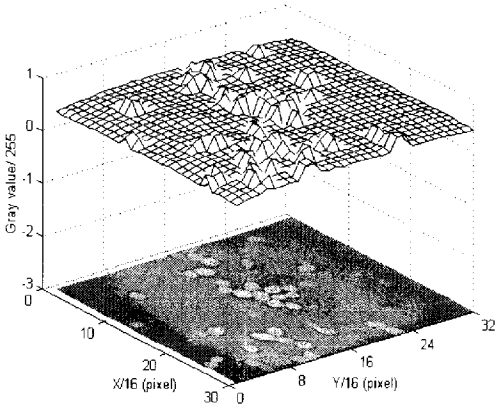

Fig. 3 The spatial representaion of gray value for the image shown in Fig. 2

This is useful to get reasonable ways to apply 2-dimensional signal processing technique based on linear theory. The microscopic image often has several special properties such as non-symmetric contour, a bimodal histogram, and multi-layer objects, etc. Non-symmetric contour is due to light source of the microscope concentrated on the center of the image. Luminance at the center of the

background is higher than that of its surrounding. This property affects a gray-level histogram of the image. Therefore, to see more clearly the target cells, it is more desirable to get rid of the noise from background. So, the aim of this paper is to propose an algorithm that can separate the target cells exactly under background with noise.

2.3 Morphological Feature Extraction of Microorganisms

Pattern recognition based on statistical decision rule has three stages such as image segmentation, feature extraction and classification in Fig. 4.

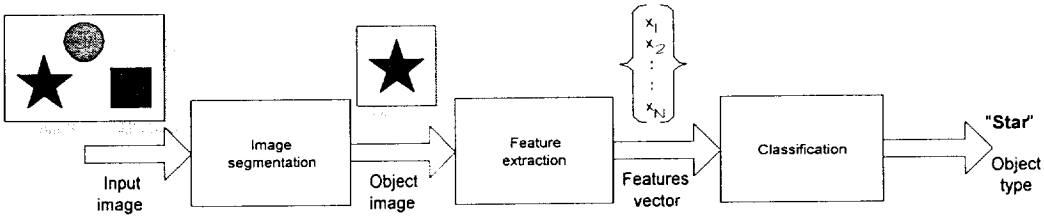

Fig. 4 The three phases of pattern recognition

First, pre-filters improve the quality of the acquired original image so that general noise is eliminated, and objects in the image are clearer than the prior. After preprocessing, image segmentation phase based on Otsu's optimal threshold selection makes binary image from gray-level image. Threshold plays a role in the critical point to separate objects from background. Next, several binary morphological filters such as cleaning, opening and filling filters get rid of isolated particles. And then, the labeling algorithm segments each objects by 4-adjacent neighborhood as shown Fig. 5(a). Finally, morphological feature vectors such as area, perimeter, complexity, centroid, rotation angle, width, height and effective diameter are extracted by the binary image processing.

Feature vector extraction is to extract a set of the elementary properties to quantify some significant characteristics of the object. Because the classification of object type is based on these feature vectors, feature parameters must be selected as cautious as possible. If feature vectors are decided irrationally, error rate in misclassifying objects is increased.

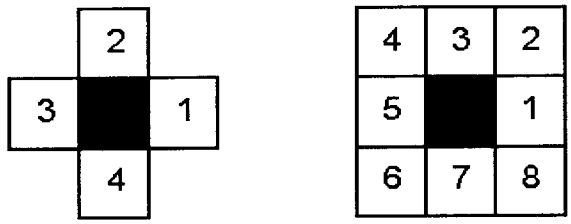

(a) 4-adjacent (b) 8-adjacent

Fig. 5 Neighborhoods

2.3.1 Pre-filters and Image Segmentation

In this chapter, morphological filters are applied such as opening, cleaning, etc. Image segmentation is a fundamental technique for image analysis, whose purpose is to identify the regions of image objects and to extract the objects from their background[2]. This paper engages *Otsu's variance based thresholding method* in Appendix 1[6]. He described three possible discriminant criteria based on ratios of the within-class, between-class and total variance, all of which are equivalent, and thus in a given situation any of the three possible discriminant criteria could be chosen[1]. In general case, threshold value is chosen to maximize the between-class variance because it makes the simple calculation.

2.3.2 Feature Vector Extraction

In Fig. 6, feature vector is determined to identify object as follows:

$$F \equiv [A\ L\ e\ I_C\ \theta\ W_x\ W_y\ d_e]^T \tag{2.1}$$

where A is area of each labeled object, L is the length of perimeter, (I_C, J_C, θ) are centroid of the object and primary angle of its axis, (W_x, W_y) are the width and the height. The effective diameter d_e is a diameter of the object that is considered as circle.

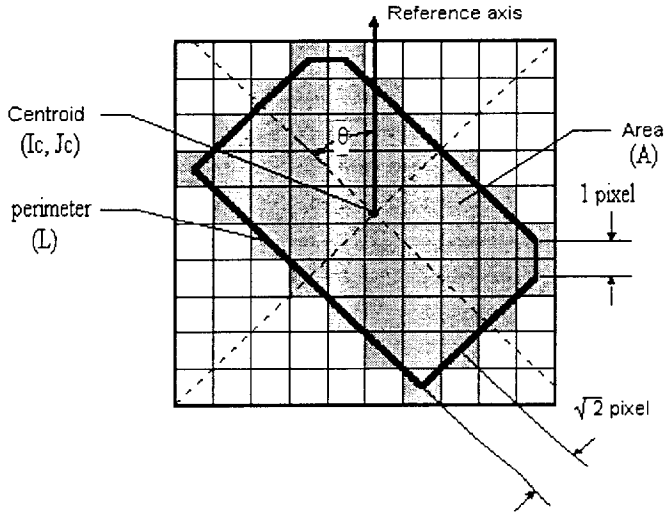

Fig. 6 Concepts of moment and geometric parameters

The object area A is calculated by summing pixels in the image as follows:

$$A = \sum_{i=0}^{M} \sum_{j=0}^{N} f(i, j) \tag{2.2}$$

$f(i,j)$ is a binary image that has 1 inside object and 0 inside background and $M \times N$ is a size of an image.

The perimeter L is obtained by counting boundary pixels, where the distance between 8-adjacent pixels is 1 or $\sqrt{2}$ pixel unit. Using chain code with 8 directions shown as Fig. 5(b), L is calculated as follows:

$$L = m + \sqrt{2}n \tag{2.3}$$

where m is the number of odd number and n is the number of even number in chain code.

Simply counting boundary pixels cannot make reasonable result. Therefore, the directions of the boundary must be kept to the tracks of the path. Complexity of the object is taken as following:

$$e \equiv \frac{L^2}{A} \tag{2.4}$$

Morphological features of shapes include the moment parameters as follows:

$$M(p,q) \equiv \sum_{(i,j)} i^p j^q f_{ij} \tag{2.5}$$

There are several parameters to be calculated by combinations of Eq. (2.5). However, in this paper, the centroid (I_c, J_c), central moments μ_{ij} taken the center of gravity as the origin and the rotation angle θ are only measured as follows:

$$I_C = \frac{M(1,0)}{M(0,0)} \tag{2.6}$$

$$J_C = \frac{M(0,1)}{M(0,0)} \tag{2.7}$$

$$\mu_{ij} = \sum_{i=0}^{M} \sum_{j=0}^{N} (i - I_c)^i (j - J_c)^j f(i,j) \tag{2.8}$$

$$\tan\theta = \frac{2\mu_{11}}{\mu_{20} - \mu_{02}} = \frac{-M_0 \pm \sqrt{M_0^2 + 4}}{2} \tag{2.9}$$

where

$$M_0 \equiv \frac{M(2,0) - M(0,2)}{M(1,1)} \tag{2.10}$$

The width W_x and W_y are determined by measuring the distances between each first detected pixels from left, right, top, and bottom side after rotating the object region for the rotation angle θ obtained from Eq. (2.9). The width and height is measured after the clock-wise rotation step using rotation transformation matrix T as follows:

$$T = \begin{bmatrix} \cos\theta & -\sin\theta \\ \sin\theta & \cos\theta \end{bmatrix} \tag{2.11}$$

$$W_x = \text{rightmost pixel - leftmost pixel} \tag{2.12}$$

$$W_y = \text{bottommost pixel - topmost pixel} \tag{2.13}$$

The effective diameter d_e^2 can be defined as follows:

$$\pi d_e^2 = A \tag{2.14}$$

2.3.3 Flowchart for Proposed Method

Fig. 7 shows the flowchart for proposed method.

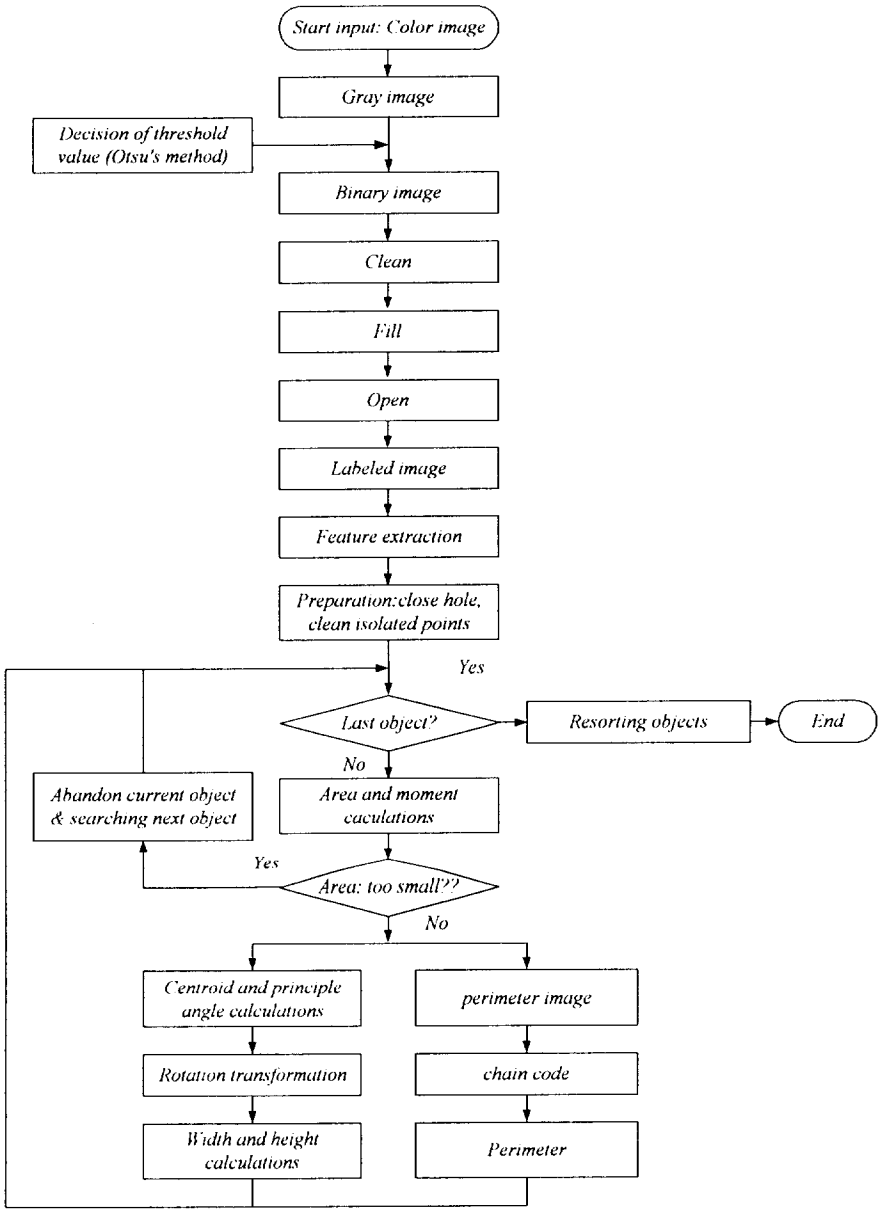

Fig. 7 Flowchart for extractions of moment and geometric parameters

The proposed procedure includes area filter to cancel next extraction procedure for very small object in order to obtain higher calculation efficiency than the method using only Otsu's method.

The preparation step in the flowchart also contains several filters based on binary morphological procedure such as filling hole and cleaning isolated point.

2.4 Experiment results

Fig. 8 shows the theshold criterion(J) and the optimal threshold value obtained by Otsu's method in Appendix 1. The optimal threshold for the image was determined as $t = 102$ at $J_{max} = 0.556025$. The result graph is shown in Fig. 9.

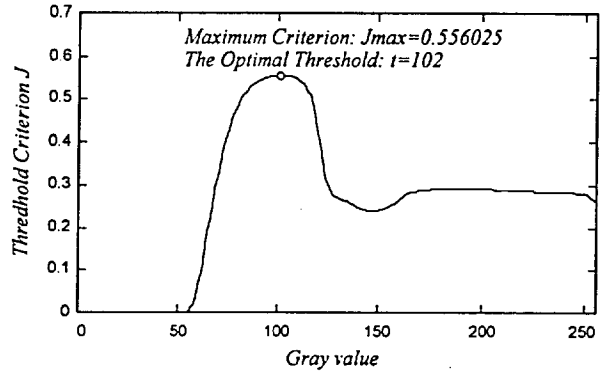

Fig. 8 Otsu's optimal threshold selection for Fig. 10(a)

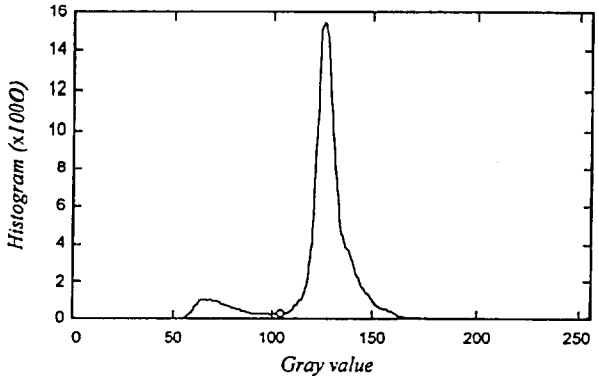

Fig. 9 Histogram and thresholding value for image Fig. 10(a)

Fig. 10 shows the image processing results obtained by the proposed method. In Fig. 10, (a) shows the original image as shown in Fig. 2, (b) is a binary image obtained by thresholding value, $t = 102$, (c) is an image obtained after removing the isolated object and filling holes in the binary image(b) and (d) shows an image obtained by filtering area less than pre-described pixels in the filtered image(c).

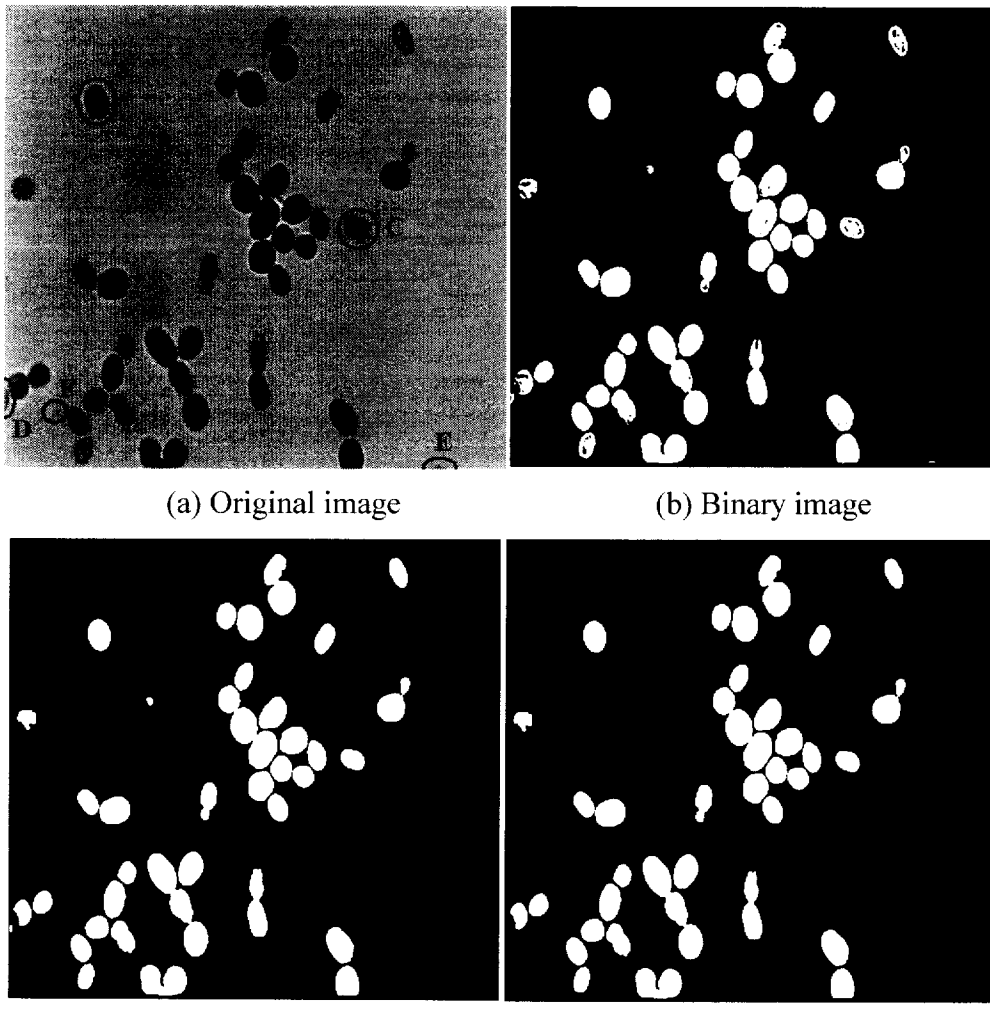

(a) Original image (b) Binary image

(c) Filtered image (d) Final image

Fig. 10 Image processing results obtained by the proposed method

Fig. 11 describes the labeled images of Fig. 10. In Fig. 11, (a) is a labeled image obtained by only Otsu's method. (b) is a labeled image obtained after cleaning, filling and opening filters and (c) are labeled images obtained after filtering area less than pre-described pixels by the proposed method.

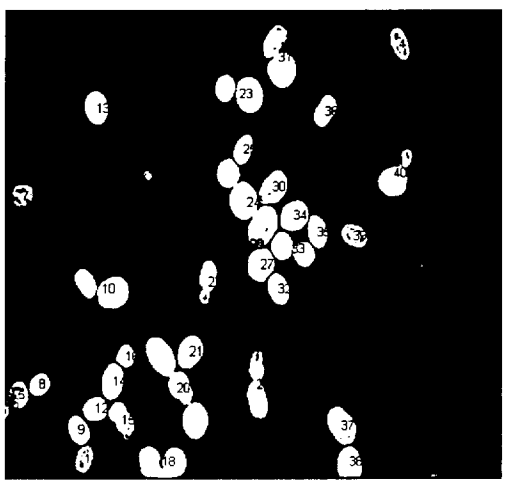

(a) Only Otsu's method

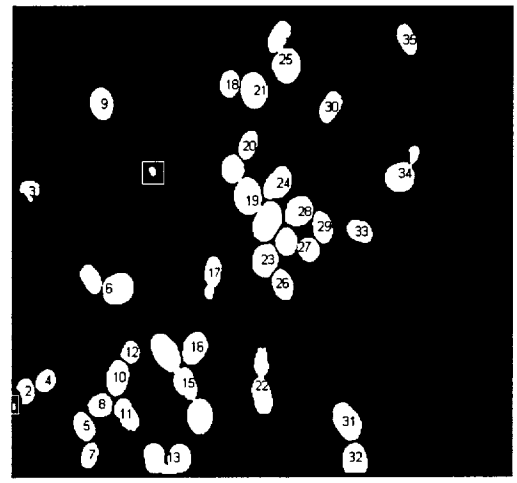

(b) Opening, cleaning and filling hole

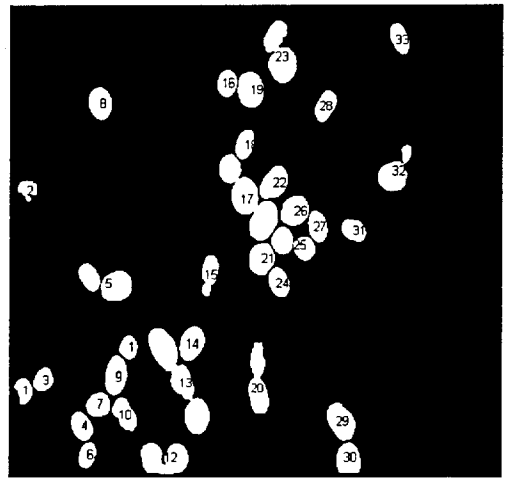

(c) Proposed method

Fig. 11 Labeled images

The counted numbers on the labeled images in Fig. 11 represent the number of labeled microbial cells. We can find that some cells have holes by only Otsu's

method in Fig. 11(a), especially, such as non-focused cells like 'C' or are not detected like 'F' in Fig. 10(a). Fig. 11(b) shows that many cells are eliminated from Fig. 11(a) by canceling isolated points and filling holes by morphological filters such as cleaning, filling, and opening filters. Fig. 11(c) shows that marked cells(□) in Fig. 11(b) less than the area of prescribed pixels are erased by area filter. After labeling objects as shown in Fig. 11(c), feature extraction vectors such as area, perimeter, complexity, centroid, rotation angle and effective diameter are done.

Fig. 12 shows the area distributions of Fig. 11(b) and Fig. 11(c). In Fig. 11(c), the cells of the areas marked by □as shown in Fig. 12 are removed.

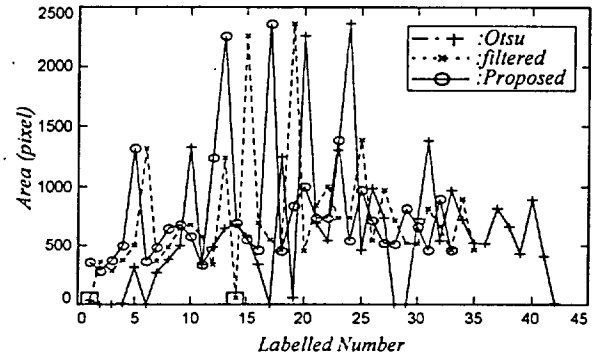

Fig. 12 Area plot after labeling

Fig. 13 shows sampled images from Fig. 11(a). Fig. 14 describes the same images as Fig. 13 sampled from Fig. 11(c). They include two ellipsoidal objects((a) and (d)) and two overlapped images((b) and (c)) in Fig. 13 and Fig. 14.

Fig. 13 Example images by only Otsu's

Fig. 14 Example objects method by the proposed method

Fig. 15 shows perimeter image and rotation process. In Fig. 15, (a) is labeled image, (b) is perimeter image and (c) is rotated image.

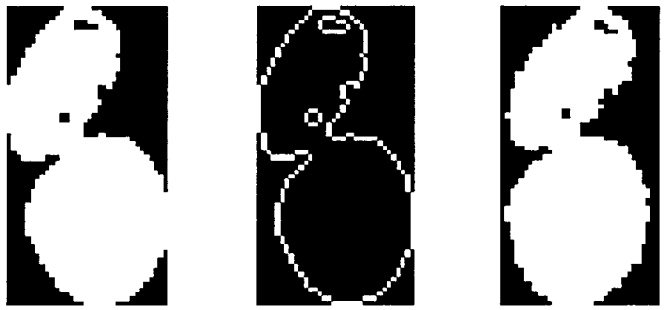

(a) Labeled image (b) Perimeter image (c) Rotated image

Fig. 15 Perimeter image and rotation process

With chain code of Fig. 15(b), the perimeter of labeled image(a) is measured by Eq.(3.3). First, we make perimeter image(Fig 15(b)) from the labeled image(Fig. 15(a)) to produce the chain code. We find the first pixel of the perimeter image and start the first pixel in the counter-clockwise direction. The direction numbers(Fig. 5(b)) along the perimeter as shown in Fig. 15(b) become chain code as following:

Chain code of Fig. 14(d)= 66667676676676776777777787878818112
1222223223223233233233343334444455555

$$L = \sqrt{2} \times even + odd$$

From the rotated images(Fig. 15(c)) that the labeled images(Fig. 15(a)) are rotated by rotation angle θ in the clock-wise direction, widths and heights of the labeled images are measured by Eqs.(2.12) and (2.13). The feature vectors of the selected example objects are obtained from Eqs.(2.1)–(2.14) as the following Table 1 by Otsu's method and Table 2 by the proposed method respectively.

Table 1 Feature vectors of selected e example objects by only Otsu's method

Object	A	L	e	(I_c, J_c, θ)	(W_x, W_y)	d_e
Unit	pixel	pixel		(pixel, pixel, ∘)	(pixel, pixel)	pixel
a	647	103.54	16.57	(17.48, 12.67, 8.36)	(24, 34)	28.70
b	1243	202.7	33.1	(18.3, 24.7, -2.3)	(49, 33)	39.8
c	1357	200.1	29.1	(34.9, 16.9, 11.7)	(31, 64)	41.8
d	516	88.74	15.26	(16.70, 11.65, -22.96)	(23, 30)	25.63

Table 2 Feature vectors of selected e example objects by the proposed method

Object	A	L	e	(I_c, J_c, θ)	(W_x, W_y)	d_e
Unit	pixel	pixel		(pixel, pixel, ∘)	(pixel, pixel)	pixel
a	647	103.54	16.57	(17.48, 12.62, 8.36)	(24, 34)	28.70
b	1242	203.6	33.4	(17.3, 24.7, -2.2)	(49, 32)	39.8
c	1383	200.8	29.1	(34.7, 16.9, 11.6)	(31, 64)	42.0
d	516	88.74	15.26	(16.70, 11.65, -22.96)	(23, 30)	25.63

Feature vectors of simple ellipsoidal objects having no hole or few holes such as (a) and (d), by only Otsu's method and by the proposed method are same, but the feature vectors of objects having a lot of holes such as (c) and having complex shape such as (b) by only Otsu's method and the proposed method is different. Because feature vectors are affected by noises and holes as well as shape, it is necessary to remove noises contaminated in original image to get feature vector extraction exactly.

2.5 Conclusion Remarks

This paper shows basic research results to develop vision analysis system which can be applied for bioprocess plant and to present a procedure extracting features

in order to identify the object cells exactly under background with noise such as obstacles and non-symmetric contour, etc. To prove the effectiveness, the proposed method is applied for yeast, *Zygosaccharomyces rouxii.* The segmented image by only Otsu's method includes holes and noises, but the segmented image by the proposed method is clearer than that by only Otsu's method. We can see that the feature vector is affected by holes, noises and shape. We can also see that extracting the feature vector such as area, perimeter, complexity, centroid, rotation angle, width, height and effective diameter obtained by proposed method is more exact and more efficient to express geometric information of the cell than that obtained by only Otsu's method.

III

Reconstruction and Elimination of Optical Microscopic Background Using Surface Fitting Method

3.1 Introduction

The work observing objects through a microscope is not only tedious but also iterative. From 1960, these kinds of works are automated by using image processing technique and nowadays, the image analysis system is regarded as a necessary device for the optical microscopes[9]-[14]. In cell engineering, digital image analysis is applied for several application fields. Pons et al. used a semi-auto image analysis system and analyzed morphological characteristics[12]. Zalewski proposed an on-line monitoring system that monitors elements of circumstance in culturing yeast by using general optical microscope[9]. Suhr et al. developed in-situ microscope that can analyze cell growth on-line[14]. Bloem et al. proposed a method detecting position and number of bacteria in solid foods automatically[10]. The above stated studies need a procedure extracting characteristic information of each cell in order to estimate the growth state of cells. To extract the characteristic vectors of cells, separating work of the target object and its background in microscope image is very important. In the case of optical microscope, a background that is not distributed with constant gray-level causes variation of pure gray level for cells. The traditional methods to remove the background use a concept that after acquiring only the part of background in the

captured image and storing it as a background image, they subtract the prestored background image from an obtained cell image[12]. This concept is applicable only in the state of off line. In the case of on-line analysis system, in order to consider the parameter variations of image, a complicate analysis algorithm must be realized[10, 14]. But those kinds of methods cannot be realized easily in the fields of requiring a real time processing because of its long processing time.

In this chapter, using high order surface fitting and interpolation, a background elimination method interpolating an image with unnecessary background element is proposed. The method obtains background data and reconstructs the background by calculating surface function minimizing least square error of the sampled data. It eliminates its background from the original image. Optimal thresholding elects pixels to be representative of the background and bilinear interpolation finds non-deterministic background pixels among the sampled pixels. Reconstruction procedure makes a contour image from surface function that was composed by the 2D cubic fitting method from pivoted background pixels. Elimination procedure subtracts the approximated background from the original image. When this algorithm is applied to yeast *Zygosaccharomyces rouxii* and ammonia-oxidizing bacteria *Acinetobacter* sp., the higher order surface fitting method can eliminate background suitably and estimate the object more precisely and obviously. Furthermore, we can see that it is more effective for the reduction of noise.

3.2 Reconstruction and Elimination of Background Image

Fig. 16 shows original image of (a) *Zygosaccharomyces rouxii*, a kind of yeast and (b) *Acinetobacter* sp., a kind of ammonia-oxidizing bacteria. An image variation by this kind of non-uniformed background is easily found in microscope image because intensity for center of optical light is stronger than that of its outside. According to going from center to its outside, its intensity is slowly

decreased. The non-uniformed property causes a distortion for internal gray level of object separated from background in image. In a distribution device using image processing or in application field identifying growth characteristics of microbial cells, since the internal gray level embeds the characteristics of an object such as density, color, and depth etc., the slope of background must be compensated before the parameters of the image is measured.

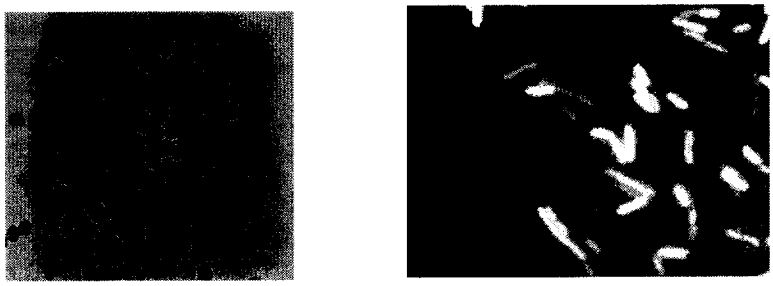

(a) *Zygosaccharomyces rouxii* (b) *Acinetobacter* sp.

Fig. 16 Original image

3.2.1 Two-dimensional 3rd Order Surface Data Fitting Technique

In this chapter, it is assumed that the background of microscope image has non-uniformed property, and its surface slope can be expressed by 3rd order polynomial. Then, we partition the captured image in a constant interval, obtain the gray level representing its background, and decide an approximate function minimizing square error of these pixels. Also it is assumed that the approximated background function $f(x, y)$ is given by the following:

$$f(x,y) = c_0 + c_1 x + c_2 y + c_3 xy + c_4 x^2 + c_5 y^2 + c_6 x^2 y + c_7 xy^2 + c_8 x^3 + c_9 y^3 \quad (3.1)$$

where c_0, c_1, ... , c_9 are coefficients of polynomials decided by least square method. Since 2nd order data fitting can be easily realized by matrix based calculation,

using a matrix B expressing polynomial according to coordinate (x, y) of background pixels, column vector Y with gray level of background pixels and column vector C of coefficients decided by least square method, a column vector E meaning an error between practical background pixel value and its approximated value can be given by:

$$\mathrm{E} = \mathrm{Y} - \mathrm{F} \tag{3.2}$$

where $\mathrm{F} = \mathrm{BC}$ means background pixel value approximated by Eq.(3.1) and subscripts M, N are sizes of data sampling for x and y axes respectively.

$$\mathrm{Y} = \begin{bmatrix} g_{11} \\ \vdots \\ g_{1N} \\ \vdots \\ \vdots \\ g_{MN} \end{bmatrix}, \ \mathrm{C} = \begin{bmatrix} c_0 \\ c_1 \\ \vdots \\ c_9 \end{bmatrix}, \ \mathrm{B} = \begin{bmatrix} 1 & x_1 & y_1 & x_1 y_1 & \cdots & x_1 y_1^2 & x_1^3 & y_1^3 \\ 1 & x_1 & y_2 & x_1 y_2 & \cdots & x_1 y_2^2 & x_1^3 & y_2^3 \\ \vdots & \vdots & \vdots & \vdots & \cdots & \vdots & \vdots & \vdots \\ 1 & x_M & y_1 & x_M y_1 & \cdots & x_M y_1^2 & x_M^3 & y_1^3 \\ \vdots & \vdots & \vdots & \vdots & \cdots & \vdots & \vdots & \vdots \\ 1 & x_M & y_N & x_M y_N & \cdots & x_M y_N^2 & x_M^3 & y_N^3 \end{bmatrix}$$

where g_{ij} is a gray level of pixel(i, j) of sampled background pixels with the size of $M \times N$.

The least square performance function of column vector E is given by:

$$\eta = \frac{1}{MN} \mathrm{E}^T \mathrm{E} \tag{3.3}$$

Substituting Eq.(3.3) into Eq.(3.2) and equaling zero for equation obtained by differentiating for C, then the result is yielded as:

$$C = \left[B^T B\right]^{-1} B^T Y \tag{3.4}$$

where the coefficient vector C minimizes the square error, and square matrix $[B^T B]^{-1} B^T$ is a pseudoinverse of B[11].

3.2.2 Interpolation of Blank Region

The interpolation means a procedure to extract background from original image after obtaining mask image. Then using mask image the part shaded by mask is regarded as a part of object and it is excluded in the procedure detecting the background. When we extract the background value, since the input image is divided as 20×15 regions with 32×32 grids, the background value of each region is given as minimum gray level in its region. Because object size is larger than grid size, there are regions in which we cannot choose the background value. We grade the regions as blank regions and the representative value is estimated using interpolation method based on neighborhood background value. Then the matrices B and Y to be used for psudoinverse calculation of Eq.(3.4) have dimensions $\Re^{MN\times 1}$ and $\Re^{MN\times 10}$ respectively. In the case that we cannot obtain the background value because all the regions are shaded by object, we use the interpolation method usually. The region of O in Fig. 17 is one which we can decide a background value by mask of object.

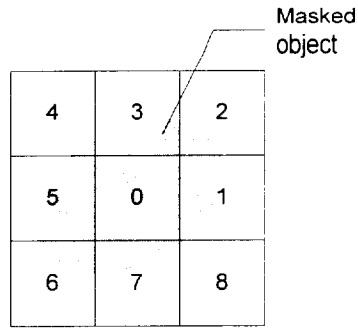

Fig. 17 A blank region problem of big masked object

The value of this region can be decided by applying bilinear interpolation method based on background values of 1~8 in Appendix 1.

3.2.3 Mask Image and Labeling

Generally, mask image can be obtained just by binarization procedure. The labeling is a basic procedure for image recognition. Since our work is a pre-stage for image analysis, we extract the mask image from label image. In the labeling procedure, an adaptive binarization procedure and a morphological filtering procedure are included. Then, isolated points and holes in object are eliminated. So, it is compatible for use of mask image[13].

3.2.4 Compensation of Image Using Background Elimination

The frame image has size of 640×480 pixels and each pixel has 256 gray levels. In order to prove the effectiveness of the proposed background compensation, we used *Acinetobacter* sp. and *Zygosaccharomyces rouxii*. The practical experimental procedure is divided by 3 steps.

[Step 1] Preprocedure: Input image to apply background algorithm is produced. That is according to needs, after applying noise reduction filter, distinguishing background and object, input and mask images are produced.

[Step 2] Obtain approximate function of background $f(x,y)$. Input image has 20×15 regions separated with 32×32 grids. The procedure of surface fitting is as follows; select one gray level representing the background in each region and get the $f(x,y)$. Using mask image the region including only object is set by blank. Using approximate function $f(x,y)$, produce approximate

background image of 640×480 pixels, and the blank region is compensated using interpolation method.

[Step 3] Background: subtracting the approximate background image from original image a compensated image is obtained. But since the compensated image has low gray level over all images, appropriate gray level compensation is realized.

Fig. 18 shows the flowchart of the reconstruction and elimination of background proposed in this chapter.

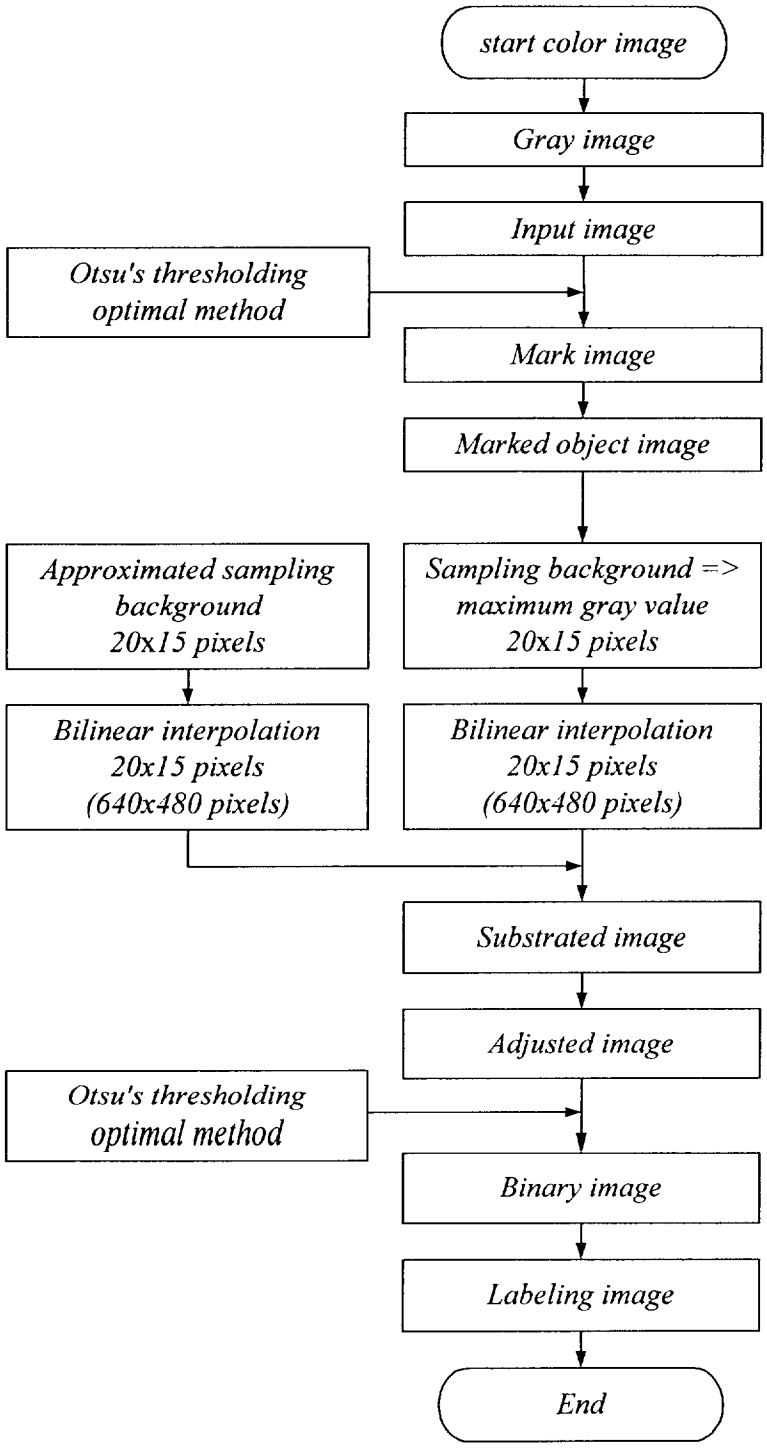

Fig. 18 Flowchart of proposed method

3.3 Experimental results and Discussion

Fig. 19~Fig. 28 show the experimental results applied to *Zygosaccharomyces rouxii and Acinetobacter* sp. using the proposed background interpolation method.

Fig. 19 and Fig. 22 show us a principle eliminating a background with slope in original images(Fig. 19(a) and Fig. 22(a)), respectively. Fig. 19(a) and Fig 22(a) are input images with shaded-background of gentle slope for *Zygosaccharomyces rouxii* and *Acinetobacter* sp. respectively. Fig. 19(b) and Fig. 22(b) show masked images extracted from original images, respectively. Fig. 19(c) and Fig. 22(c) are sampled background images from masked images(Fig. 19(b) and Fig. 22(b)), respectively. Fig. 19(d) and Fig, 22(d) are approximated background images of Fig. 19(c) and Fig. 22(c), respectively. Fig. 19(e) and Fig. 22(e) are subtracted images that the approximated background images(Fig. 19(d) and Fig. 22(d)) are subtracted from the original images, respectively. Fig. 19(f) and Fig. 22(f) are adjusted images that highlight Fig. 19(e) and Fig. 22(e), respectively. Original images(Fig. 19(a) and Fig. 22(a)) are contaminated with a background images(Fig. 19(d) and Fig. 22(d)) with a slack slope, respectively.

Fig. 20 shows histograms of Fig. 19(a), Fig. 19(e) and Fig. 19(f) for *Zygosaccharomyces rouxii.*

Fig. 23 shows histograms of Fig. 22(a), Fig. 22(e) and Fig. 22(f) for *Acinetobacter* sp.

Fig. 21 and Fig. 24 display sampled background's gray level(a) and approximate background's gray level(b) into three dimensional method that are taken with maximum gray value from Fig. 19(a) and Fig. 22(a), respectively. We can see that the backgrounds contain a lot of noise in Fig. 19(a) and Fig. 22(a), respectively.

Fig. 25(a) and Fig. 26(a) show labeled images by only Otsu's method without applying the proposed method for Fig. 19(a) and Fig 22(a), respectively. Fig 25(b)

and Fig. 26(b) are labeled images by the proposed method for Fig. 19(a) and Fig. 22(a), respectively.

Fig. 27 and Fig. 28 show the area distribution of the labeled images by Only Otsu's method and the proposed method for Fig. 19(a) and Fig. 22(a), respectively. It is shown that labeled images by only Otsu's method contains a lot of noise, while labeled images by the proposed method remove some noise as shown in Fig 25-Fig. 28.

We can also see that the proposed method remove noises from original image contaminated with noises when we compare Fig. 19(a) and Fig. 22(a) with Fig. 19(f) and Fig. 22(f), respectively.

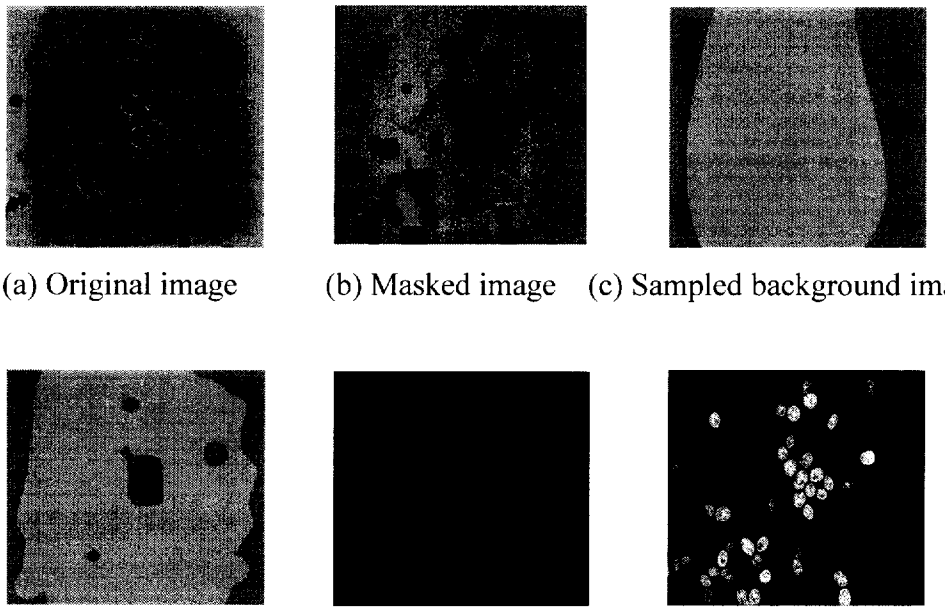

(a) Original image (b) Masked image (c) Sampled background image

(d) Approximated background image (e) Subtracted image (f) Adjusted image

Fig. 19 Resulted images for *Zygosaccharomyces rouxii*

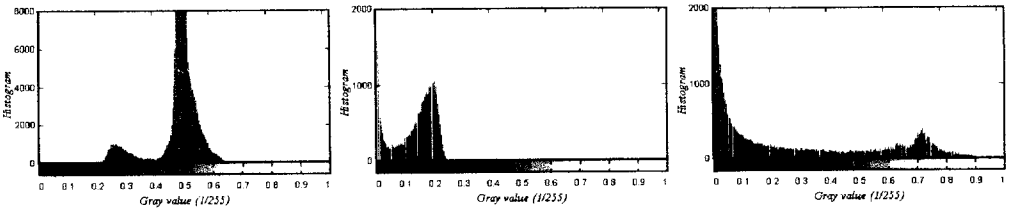

(a) Original image (b) Subtracted image (c) Adjusted image

Fig. 20 Background's gray-level for *Zygosaccharomyces rouxii*

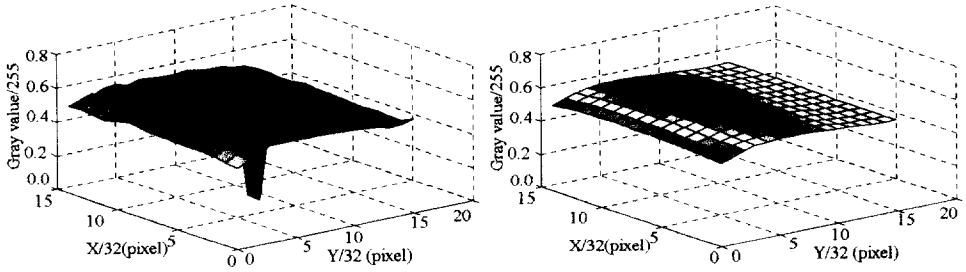

(a) Sampled (b) Approximated

Fig. 21 Background's gray-level for *Zygosaccharomyces rouxii*

(a) Original image (b) Masked image (c) Sampled background image

(d) Approximated background (e) Subtracted image (f) Adjusted image image

Fig. 22 Resulted images for *Acinetobacter* sp.

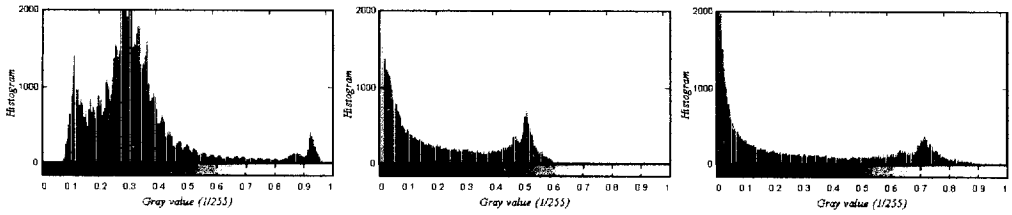

(a) Original image (b) Subtracted image (c) Adjusted image

Fig. 23 Histograms for *Acinetobacter* sp.

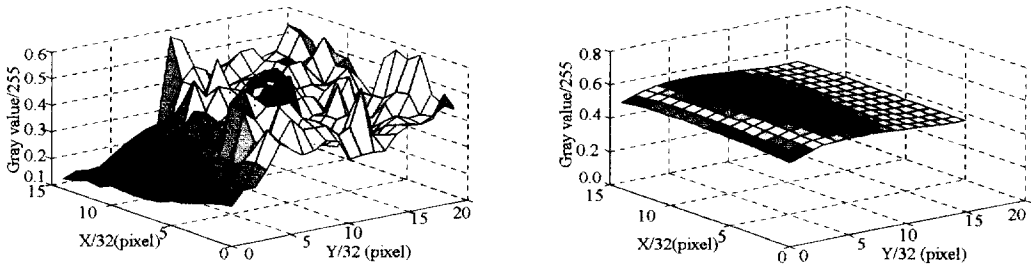

(a) Sampled (b) approximated

Fig. 24 Background's gray-level for *Acinetobacter* sp.

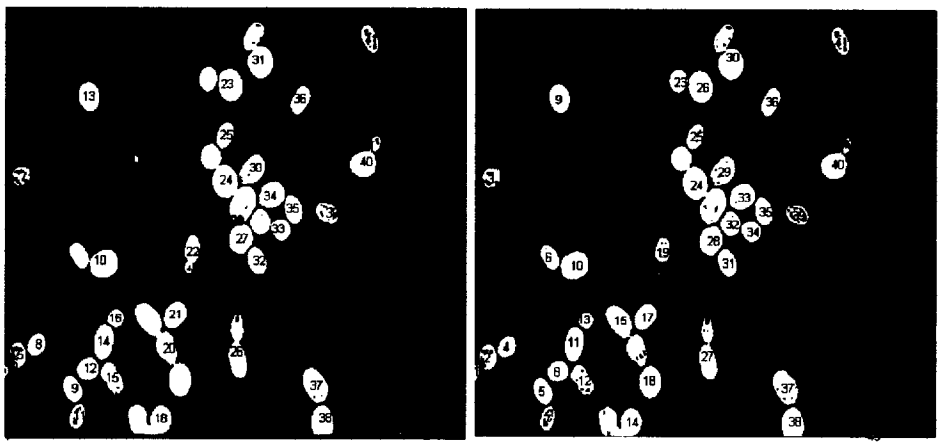

(a) Otsu's method (b) Proposed Method

Fig. 25 Labeled images for *Zygosaccharomyces rouxii*

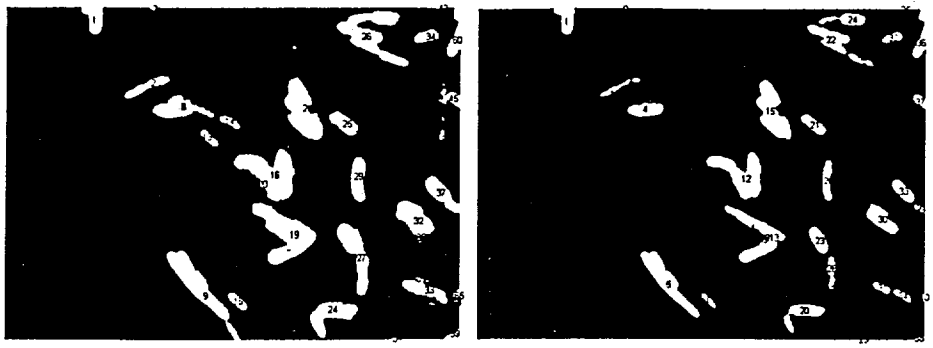

(a) Otsu's method (b) Proposed Method

Fig. 26 Labeled images for *Acinetobacter* sp.

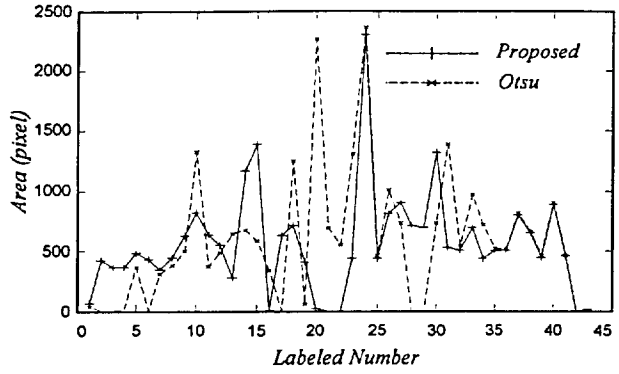

Fig. 27 The area distribution of labeled images for *Zygosaccharomyces rouxii*

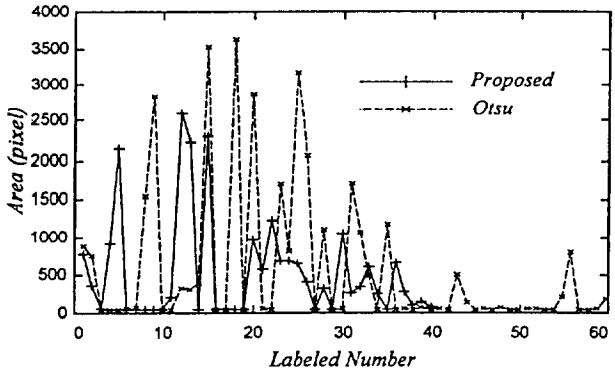

Fig. 28 The area distribution of labeled images for *Acinetobacter* sp.

3.4 Conclusion Remarks

This chapter deals with the elimination of contour background in order to get rid of the background from the input image based on a higher order surface fitting method. The elimination method used 2 dimension 3rd order surface data fitting technique and a bilinear interpolation method. The resultant compensated image is obtained through several procedures such as optimal thresholding, bilinear interpolation, reconstruction and elimination procedures. Optimal thresholding elects pixels to be representative of the background and bilinear interpolation finds non-deterministic background pixels among the sampled pixels. Reconstruction procedure makes a contour image from surface function that was composed by the 2D cubic fitting method from pivoted background pixels. Elimination procedure subtracts the approximated background from the original image. This algorithm is applied to *Acinetobacter* sp. *and Zygosaccharomyces rouxii*. The higher order surface fitting method can eliminate background suitably and estimate the object more precisely and obviously. Labeling with applying this proposed method can remove some noise and is more exact than labeling without applying this proposed method but segmentation is not satisfactory. Furthermore, it is more effective for the reduction of noise.

IV

A Segmentation Method for Counting Microbial Cells in Microscopic Image

4.1 Introduction

This chapter proposes the counting algorithms of microorganism in bioreactor and the design method of theoretical control system for controlling bioreactor system. The counting at each growing steps of microorganism is very important in order to control bioreactor system. There are a viable cell counting method using culture medium of microorganism and a direct counting method using a microscope in traditional methods for counting microorganism. A viable cell counting method has small errors. But it is too time-consuming for counting microorganisms due to cultivating them over 24 hours. A direct counting method using a microscope has large error because microorganisms are directly counted by human visual method. In case of controlling bioreactor system in a real time, a fast and precise counting method is needed since the direct counting of microorganisms by human visual method cannot be used. In case of using digital image processing method, microscopic images are obtained by interface circuit for electrical signal processing and CCD camera on microscope[15-17]. However, because the microbial cell is colorless and transparent, it must be dyed. Specially, Syto 13 is used for counting viable cells because it makes dead cell be dyed differently. But because Syto 13 not only becomes faded very fast within 2-3

seconds and the dye degree of each cell is different but also background image has different gradient, it is difficult to apply the uniform thresholding value over the entire image.

Furthermore, because binary image has a lot of overlapped image, the microcell counting methods by general segmentation method have limit to count the microbial cell exactly. So, it is necessary to develop an algorithm that can count microbial cell exactly under the condition of overlapped shape, the variation of thresholding value and various gradients of microscopic image according to the image positions.

In this chapter, a counting algorithm hybridized with an adaptive automatic thresholding method based on Otsu's method and the algorithm that elongates the markers image obtained by the well-known watershed algorithm is proposed to enhance the exactness of the microbial cell counting in microscopic images. Image thresholding is the process of classifying image gray values into two or more classes. The gray level histogram is usually the starting point for image classification. Watershed is often used in conjunction with geodesic reconstruction, a powerful tool developed by mathematical morphology, which simplifies gradient images and prevents over-segmentation. The proposed counting algorithm can be stated as follows. The transformed full image captured by CCD camera set up at microscope is divided into cropped images of $m \times n$ blocks with an appropriate size. The thresholding value of the cropped image is obtained by Otsu's method and the image is transformed into binary image. The microbial cell images below appropriately prespecified pixels are regarded as noise and removed in the binary image. The smoothing procedure is done by the area opening and the morphological filter. And then, the watershed algorithm with the proposed the elongating marker algorithm is implemented. By repeating the above stated procedure for $m \times n$ blocks, the $m \times n$ segmented images are obtained. A superposed image with the size of 640×480 pixels as same as original image is obtained from the $m \times n$ segmented block images. By labeling

the superposed image, the counting result on the image of microbial cell is achieved.

To prove the effectiveness of the proposed method in counting the microbial cell on the image, we used *Acinetobacter sp.*, a kind of ammonia-oxidizing bacteria, and compared the proposed method with the global Otsu's method, the traditional watershed algorithm based on global thresholding value and the human visual method. The result counted by the proposed method shows more approximated result to the human visual counting method than the result obtained by any other method.

4.2 Microbial Cell Counting Theory

In this section, the problems for segmenting microbial cells are presented. And then the microbial cell counting method to solve the problems is described.

To enhance the exactness to count microbial cells on the image, traditional watershed algorithm[19-20] and the proposed elongating marker algorithm that elongates the markers image obtained by the well-known watershed algorithm watershed are described.

4.2.1 Problem Statements

Because Syto13 not only becomes faded very fast within 2~3 seconds and the dye degree of each microbial cell is different but also background image has different gradient as shown in Fig. 29(a), it is difficult to apply the uniform thresholding value over the entire image. Fig. 29(b) is an image cropped from a rectangular part shown in Fig. 29(a). Furthermore, because binary image has a lot of overlapped image like Fig. 29(b), the microbial cell counting methods by general segmentation method have limit to count the microbial cells exactly.

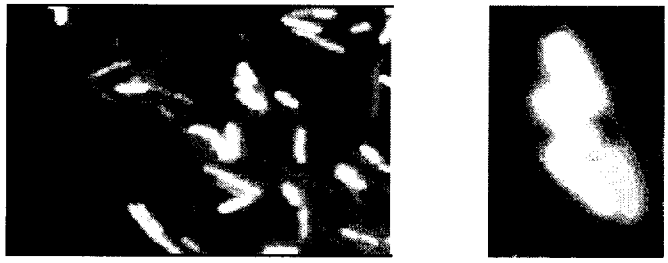

(a) Gray image (b) Overlapped image

Fig. 29 Gray image and overlapped image

Fig. 30 shows the gray value distribution for the gray image of Fig. 29(a). Fig. 31 expresses the threshold values obtained through Otsu's method for full image of Fig. 29(a) and for block by block when the full image of Fig. 29(a) is separated as 2 x 2 blocks. As we can see from Fig. 32, we can see that the thresholding values are different according to the block positions of the image. Therefore, to get more precise counting result for microbial cells, it is more desirable to obtain the thresholding value for the separated blocks rather than for the global image.

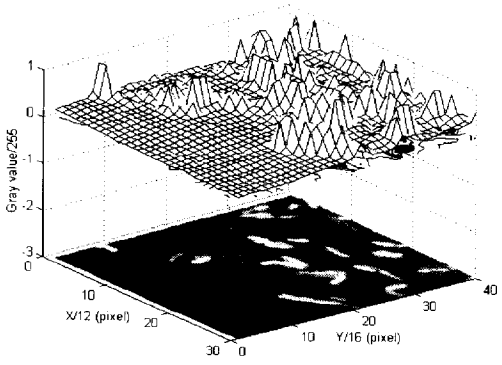

Fig. 30 The gray value distribution of Fig. 29(a)

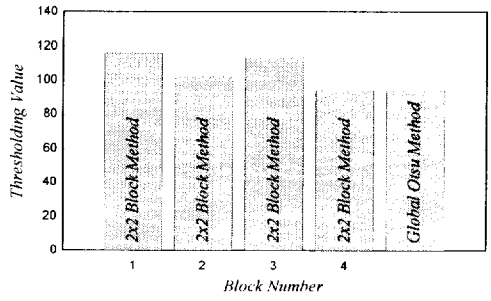

Fig. 31 Threshold values of the blocks

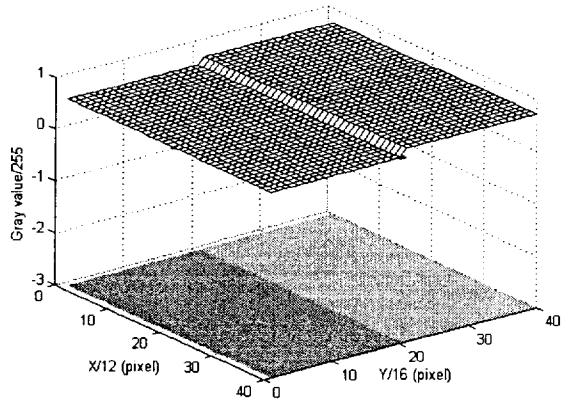

Fig. 32 Three-dimensional thresholding value of each block

So, the purpose of this chapter is to develop an algorithm that can count microbial cells exactly in spite of the overlapped shape, the variation of thresholding value and various gradients of microscopic image according to the image positions.

4.2.2 Proposed Microbial Cell Counting Algorithm

Fig. 33 describes the flow chart of the proposed algorithm where m and n are the number of the divided blocks for x and y coordinates.

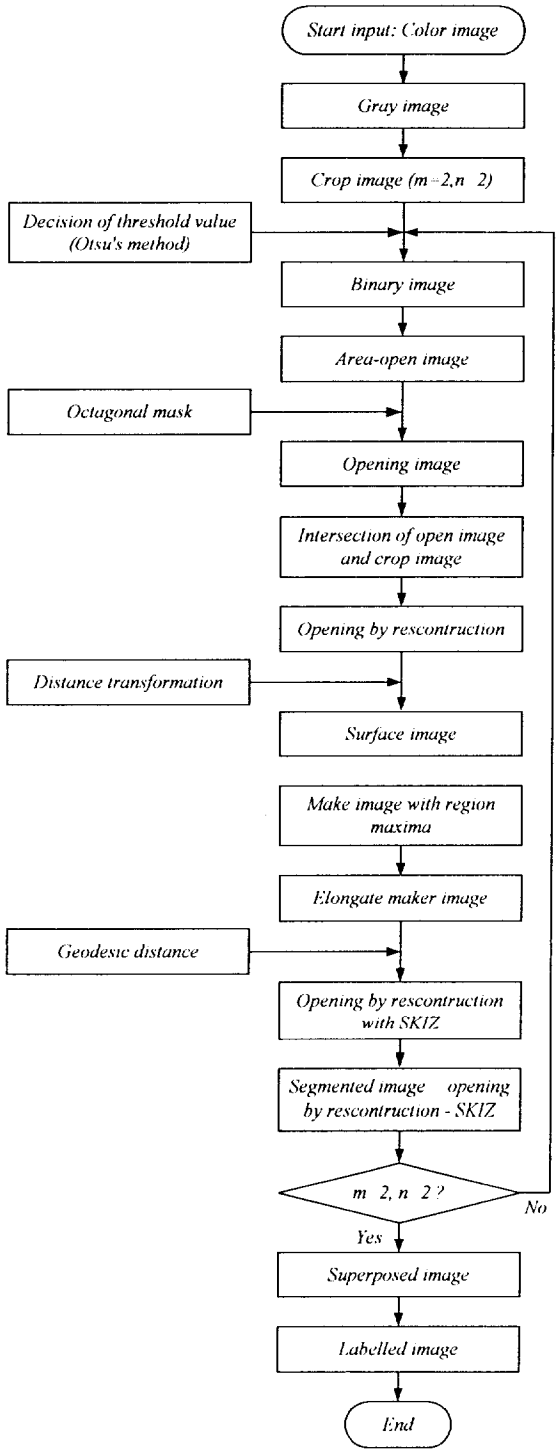

Fig. 33 The flow chart of the proposed algorithm

Because the traditional watershed algorithm produces oversegmentation, the elongating marker algorithm to solve this problem is introduced as follows:

*** Elongating marker algorithm**

function h=$elongating\ mar\ ker(f,l,\theta)$

if $|tan\theta| \le 1$

$s = sign(cos\theta)$

$x_1 = 0 : s : \text{round}(l\ cos\theta) - s$

$x_2 = round(x_1\ tan\theta)$

else

$s = sign(\sin\theta)$

$x_2 = 0 : s : \text{round}(l\ sin\theta) - s$

$x_1 = round(x_2 / tan\theta)$

end

$X_1 = max(|x_1|)$

$X_2 = max(|x_2|)$

$L_1 = 2X_1 + 1$

$L_2 = 2X_2 + 1$

$B = full(sparse(x_2 + X_2 + 1, x_1 + X_1 + 1, L_2, L_1))$

$h = open(open(f, \text{B}))$

where *round, full, sparse and max* are the functions of Matlab tool. l, θ, f and h are the length, angle of marker and marker image and elongated marker image. Function $open(f,B)$ is the function opening f by B. If there is no B, B is given as follows:

$$B = \begin{bmatrix} 0 & 1 & 0 \\ 1 & 1 & 1 \\ 0 & 1 & 0 \end{bmatrix}$$

*** Conventional Watershed Algorithm**

For the purpose of segmentation, we present here the conventional algorithm for computing the watershed, in the case of a function defined in R^2 on a digital grid, with discrete range of step functions[19-20]. A gray-tone image can be represented by a mapping function $f: Z^2 \mapsto Z$. Then $f(x)$ is the gray value of the image at point x. The points of the space Z^2 may be the vertices of a square or of a hexagonal grid. It is assumed that f is continuously differentiable. A section of f at gray level i is a set $X_i(f)$ and $Z_i(f)$ defined as:

$$X_i(f) = \{X \in Z^2 : f(x) \geq i\} \tag{4.1}$$

$$Z_i(f) = \{X \in Z^2 : f(x) \leq i\} \tag{4.2}$$

The distance function is defined by

$$\forall y \in Y, \quad d(y) = dist(y, Y^c) \tag{4.3}$$

where Y is a set of markers and is its complementary set Y^c.
A section of d at gray level i is given by

$$X_i(d) = \{y : d(y) \geq i\} = Y \ominus B_i \tag{4.4}$$

where B_i is a disk of radius, and $\ominus$ means erosion of Y.

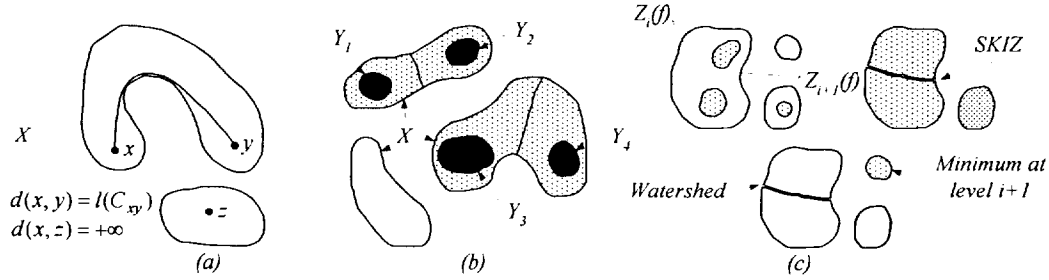

Fig. 34 (a) Shortest path and geodesic distance (b) SKIZ of a set Y in X
(c) Watershed construction using geodesic SKIZ

We can calculate the geodesic distance $d_X(x,y)$ between x and y as the length of the shortest path(if any) included in X and linking x and y as shown in Fig. 34(a).

$$\begin{cases} d_X(x,y) = \textit{shortest length}\left(C_{xy}\right) & \textit{for} \quad x,y \in X \\ d_X(x,z) = +\infty & \textit{for} \quad x,z \notin X \end{cases} \tag{4.5}$$

C_{xy} is all of paths linking x and y in X. Then, we calculate that the set of all points of X that are at a finite geodesic distance from Y:

$$R_X(Y) = \{x \in X;\ y \in Y,\ d_X(x,y) : \textit{finite}\} \tag{4.6}$$

Next, we obtain *SKIZ*(geodesic skeleton influence zone) of Y in X that is the boundaries between the various influence zones as shown in Fig. 34(b) and (c).

$$Z_X(Y) = \{x \in X;\ d_X(x,Y_i) : \textit{finite} \ \textit{and} \ \forall j \neq i,\ d_X(x,Y_i) < d_X(x,Y_j)\} \tag{4.7}$$

$$IZ_X(Y) = \bigcup Z_X(Y_i) \tag{4.8}$$

$$SKIZ_X(Y) = X / IZ_X(Y) \tag{4.9}$$

where $\cup$ and / stands for the set difference and union.

Finally, we build the watershed shown in Fig. 34(c) as follows: the minima of the function at height $i+1$, $M_{i+1}(f)$ and the section at level for the catchment basins of f, $W_i(f)$ are respectively given by:

$$M_{i+1}(f) = Z_{i+1}(f) \ / \ R_{Z_{i+1}(f)}(Z_i(f)) \tag{4.10}$$

$$W_{i+1}(f) = [IZ_{Z_{i+1}(f)}(X_i(f))] \cup M_{i+1}(f) \tag{4.11}$$

where $W_{-1}(f) = 0$.

At the end of the iteration process, the watershed line $WL(f)$ is equal to:

$$WL(f) = W_N^c(f) \quad (\text{with } \max(f) = N) \tag{4.12}$$

4.3 Experimental Results and Discussions

4.3.1 Experimental Condition of Medium.

Acinetobacter sp., a kind of ammonia-oxidizing bacterias[18] is used for experiment. First, we input 1.5 ℓ Bacto Nutrient Broth(Difco) in 2.5 ℓ bioreactor and sterilize them for 5 minutes at the condition of 121℃ in temperature, 15lbs/in2 in pressure. And then, we inoculate 103CFU/mℓ of *Acinetobacter sp.* in bioreactor, cultivate them at the temperature of 30℃ and agitate with velocity 7 rpm for air supply 0.4vvm, DO 0.1 and pH 6.8. We input Syto 13 into 1 mℓ

medium, mix it well and put it on the ambient air for 20 minutes. After that, by filtering through nuclepore PC membrane(ϕ 1.3 ㎝, Costar, USA) by vacuum pump, we fix the nuclepore on slide glass and observe the microscopic image. And then, we get the microscopic images by CCD camera and frame grabber card. By human visual method, we count the microbial cells on the microscopic image after blocking the image at the constant size. Finally, we store the image and compare this visual method with global Otsu's method, traditional watershed algorithm based on global thresholding value, and the proposed method.

4.3.2 Experimental Results

In this chapter, the experiment is done for the microbial cell counting algorithms such as global Otsu's method, traditional watershed algorithm based on global thresholding value, and the proposed method.

Fig. 35 shows the procedure that the proposed method is applied to microscopic image obtained from microscope.

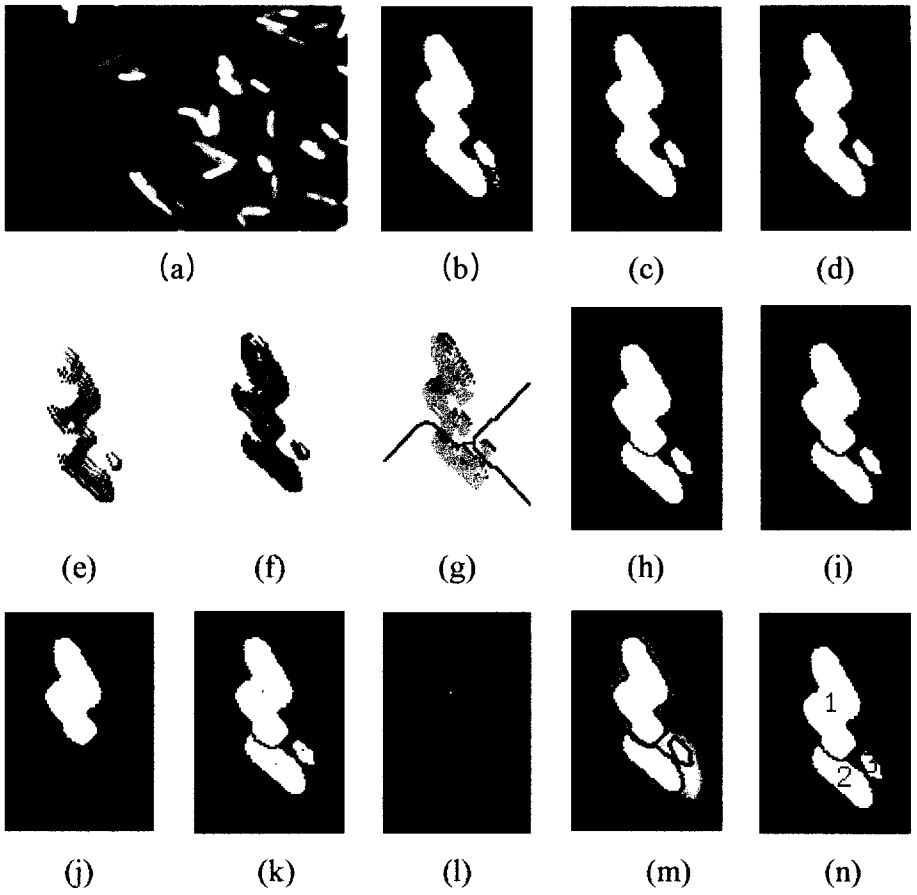

Fig. 35 The procedure of the proposed algorithm

(a) Gray image (b) Binary image (c) Areaopen image (d) Open image (e) Surface image. (f) Surface image with maxima (g) Image with watershed line (h) Image with watershed lines (i) Segmented Image (j) Labeled image (k) Labeled image with center points (l) Center points (m) Gradient image on the gray image (n) Labeling image

Fig. 36(b)~Fig. 36(l) show the results realizing the proposed algorithm for the right hand part of top after dividing Fig. 36(a) into 2×2 blocks(m=2, n=2). Fig. 36(m) and Fig. 36(n) show the results combining the cropped images into one image and labeling the microbial cells.

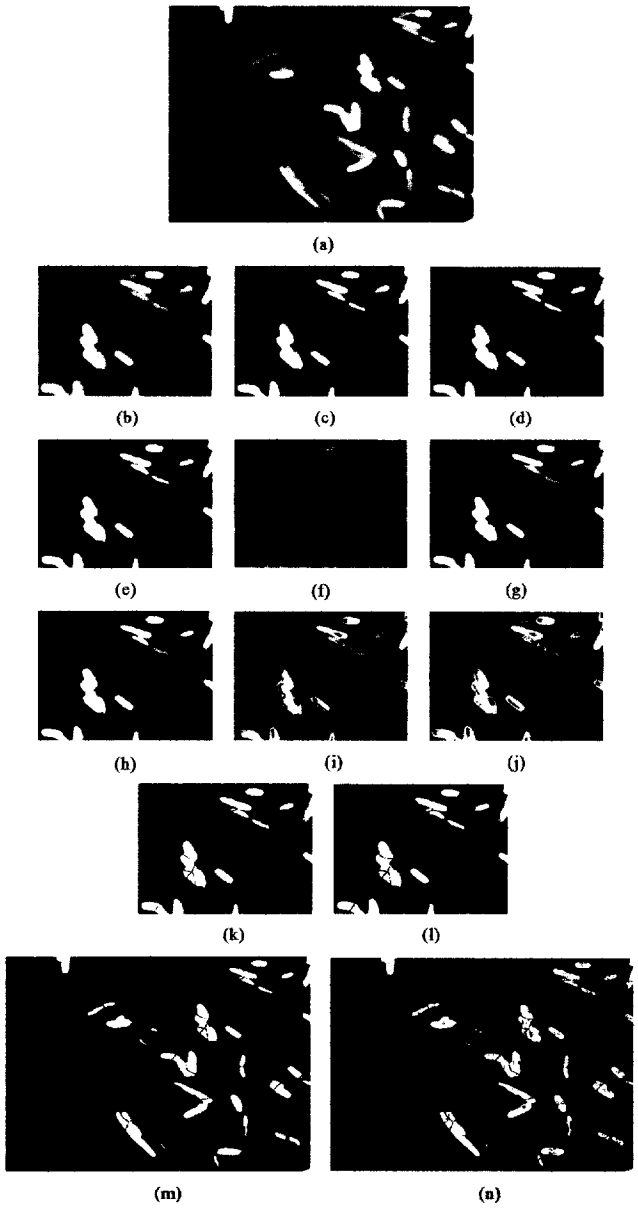

Fig. 36 The example applied to the proposed algorithm

(a) Gray image (b) Cropped gray image (c) Binary image (d) Areaopen image (e) Opening image (f) Opening image on the crop image (g) Intersection image between opening image and gray image (h) Opening image by reconstruction (i) Marker image with region maxima (j) Marker image on elongated structures (k) SKIZ image with distance transformation and watershed algorithm (l) Segmented image (m) Superposed image (n) Labeled image

Fig. 36 describes the results of reconstructing the cropped images and labeling the microbial cells. The proposed algorithm is processed as the follows. The image signals captured by CCD camera set up at microscope are changed to the corresponding digital image signals by image grabber interface card and those are saved in the frame memory. Then the saved image is color image with 640×480 pixels and it is transformed into gray image as shown in Fig. 36(a). The transformed full image is divided into cropped images of $m \times n$ blocks(Fig. 36(b)). The thresholding value of the cropped image is obtained by Otsu's method and the image is transformed into binary image based on the thresholding value(Fig. 36(c)). The area opening that the microbial cell images below appropriately prespecified pixels are regarded as noise and removed in the binary image is done (Fig. 36(d)). The smoothing procedure is done by the morphological filter(Fig. 36(e)) where the mask is a type of octagonal as the following :

$$\text{Octagonal}=\begin{bmatrix} 0 & 0 & 1 & 1 & 1 & 1 & 0 & 0 \\ 0 & 1 & 1 & 1 & 1 & 1 & 1 & 0 \\ 1 & 1 & 1 & 1 & 1 & 1 & 1 & 1 \\ 1 & 1 & 1 & 1 & 1 & 1 & 1 & 1 \\ 1 & 1 & 1 & 1 & 1 & 1 & 1 & 1 \\ 1 & 1 & 1 & 1 & 1 & 1 & 1 & 1 \\ 0 & 1 & 1 & 1 & 1 & 1 & 1 & 0 \\ 0 & 0 & 1 & 1 & 1 & 1 & 0 & 0 \end{bmatrix}$$

After catching the intersection between the opened image and the cropped gray image, the combined image as possible as similar to the original image is obtained(Fig. 36(f) and (g)). The opening image by reconstruction (Fig. 36(h)) is obtained by morphological reconstruction of the opening image[13]. The watershed algorithm is applied for the cropped block images and each microbial cell is segmented. That is, from opening image by reconstruction, we get the distance function of Eq. (4.3), the surface image(Fig. 35(e)) based on the distance function and the region maximum points that are used as markers(Fig. 36(i)) from

the surface image. Because markers produce over-segmentation, these markers are elongated in the long direction of object by the proposed elongating marker algorithm(Fig. 36(j)). The SKIZ is got from the equation of geodesic distance $d_X(x, y)$ of Eq. (4.5) based on this elongated marker images and the images with watershed lines (Fig. 36k)) are produced from the Eq. (4.12). And then, segmented images(Fig. 36(l)) are obtained by subtracting watershed lines from these images(Fig. 36(k)). We repeat the above stated procedure for $m \times n$ blocks, and the $m \times n$ segmented images are obtained(Fig. 36(l)). A superposed image (Fig. 36(m)) with the size of 640×480 pixels as same as original image is obtained from the $m \times n$ segmented block images got by repeating the previous procedure. By labeling the superposed image, the counting result on the image of microbial cells is achieved(Fig. 36(n)).

Fig. 37 shows the results that apply each algorithm. (a) shows gray image transformed from color image obtained from CCD camera, (b) shows image by global Otsu's method and (c) shows image by the global thresholding based on watershed algorithm and (d) shows image by the proposed algorithm.

Sample 1: initial state

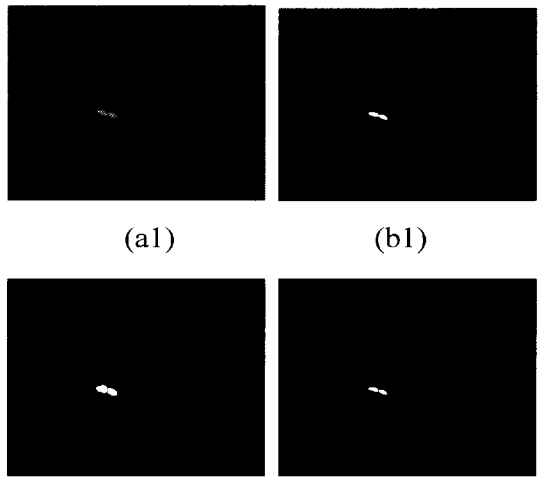

(a1) (b1)

(c1) (d1)

Sample 2: 10 times dilution after 9-hour cultivation

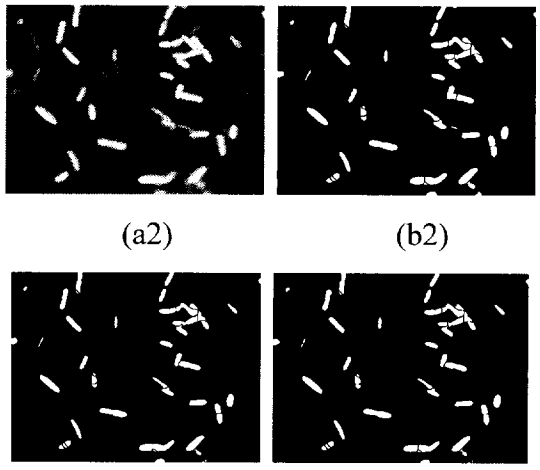

(a2) (b2)

(c2) (d2)

Sample 3: 100 times dilution after 21-hour cultivation

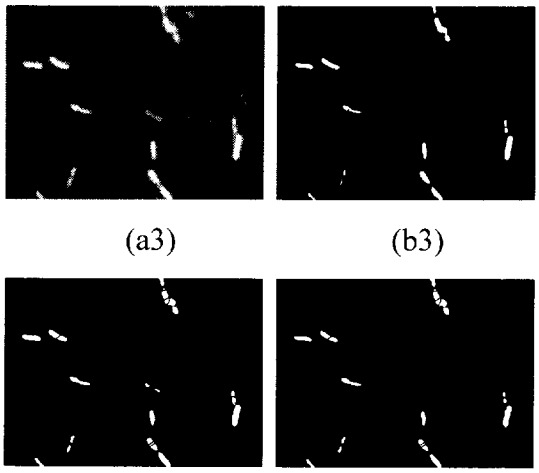

(a3) (b3)

(c) (d3)

Fig. 37 Result images

(a) Original images (b) Images by the conventional Otsu's method (c) Images by the global thresholding based on watershed algorithm (d) Images by the proposed method

Fig. 38 shows the result of labeling the images (b), (c) and (d) in Fig. 37. As shown in Fig. 38, we can see that the number of the microbial cells counted by the

proposed method shows the most approximated result to the cells counted by human visual method.

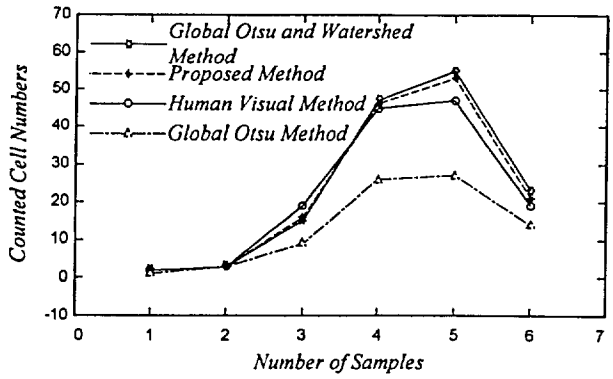

Fig. 38 Counting result of viable microbial cells

Of course, it is difficult to prove the effectiveness of the proposed method because the counting result by human visual method produces the errors depending on the counters although the cells counted by the proposed method is most approximate to the cells counted by human visual method. But because the proposed algorithm based on watershed algorithm proceeds to the segmentation similarly to counting by human visual method in spite of the overlapped image, the result is more reliable.

The denser the microbial cells are, the bigger the error between the proposed method and the other methods becomes. The density of the microbial cells and the gap of gray level between backgrounds according to the positions in an image must be small to count microbial cells exactly. To make lower the density of microbial cells, the increase of dilution rate and enough agitation must be desired. To decrease the gap of gray level on backgrounds, the development of excellent dying materials, exact dying methods, setting exact foci of lenses and removing noise are needed.

4.4 Conclusion Remarks

A counting algorithm combining an adaptive automatic thresholding method based on Otsu's method and the algorithm that elongates markers obtained by the well-known watershed algorithm is proposed to enhance the exact microbial cell counting in microscopic images. The effectiveness of the proposed method in counting the microbial cell on the image is proved using *Acinetobacter sp.*, a kind of ammonia-oxidizing bacteria, and the proposed method is compared to the global Otsu's method, the traditional watershed algorithm based on global thresholding value and human visual method. The result counted by the proposed method shows more approximated result to the human visual method than the result counted by any other method. The counting error is affected by microbial cell density and the gap of gray level in background. So to obtain more precise counting result, we need dying mycrocells exactly, the fast grasp of microscopic image, the enough agitation to have uniform distribution of microbial cells and removing background in getting images.

V

Nonlinear Adaptive Control of Fermentation Process in Bioreactor

5.1 Introduction

Because fermentation process is so complex, time varying and highly nonlinear due to biomass concentration, substrate concentration and production formulation, etc, it is difficult to make a model and control for fermentation process exactly. Specially, the exact estimate of the specific growth rate is so uncertain due to them. This uncertainty makes adaptive control theory and sliding mode method enables to be applied to fermentation process[25-33]. Miroslav Krstic applied adaptive back-stepping method for control of biochemical process with assuming of constant dilution rate and defined specific growth rate function[29]. This function includes two unknown parameters. Yet there is no way of deriving such function from the known models of specific growth rate.

It is important that the concentration of substrate in bioreactor keep constant in continuous fermentation process. In this paper, we proposed a nonlinear adaptive controller for tracking substrate concentration by manipulating dilution rate in a continuous baker's yeast cultivating process in bioreactor. Control law is obtained from Lyapunov control function to ensure global asymptotical stability of the system by using adaptive nonlinear back-stepping method. Haldane model as the specific growth rate is used. It is assumed that the specific growth rate depends

only on substrate concentration and the substrate concentration in the bioreactor and feed line are measured. Because of the uncertainty of specific growth rate, the specific growth rate can be modified as a function including the bounded unknown parameter. The deviation from the reference is observed when the external disturbance such as the change of the feed is introduced to the system. The effectiveness of the proposed controller is shown through simulation results in continuous system.

5.2 Process Model

The process considered is a continuous stirred tank in which the growth of microorganism is controlled. The bioreactor is continuously fed with the substrate influent. It is assumed that the rate of outflow is equal to the rate of inflow. The volume of culture remains culture without washout. It is considered that the feeding substrate is diluted in the water stream and the dilution rate is used as the process input. The substrate concentration is regarded as output. The system dynamic equations on the substrate and the biomass are given as the following nonlinear form[26].

$$\dot{S} = -k\mu(S)X + D(S_{in} - S) \tag{5.1}$$

$$\dot{X} = \mu(S)X - DX \tag{5.2}$$

$$y = S \tag{5.3}$$

where

X : biomass concentration in the bioreactor

S : substrate concentration in the bioreactor

D : dilution rate

μ : specific growth rate

k : known yield coefficient

y : system output

S_{in} : external inlet substrate concentration

More than 60 expressions of the specific growth rate have been suggested such as Monod', Contois', Haldane's law, etc[33]. The choice of an approximate model for μ is far from being an easy task. In our case, it is modeled by the Haldane model as the following

$$\mu = \mu(S) = \frac{k_i \mu_m S}{k_S k_i + k_i S + S^2} \tag{5.4}$$

where

μ_m : maximum specific growth rate

k_S : saturation constant

k_i : inhibition constant.

* **Control Objective and Constraints:** The control objective is to regulate substrate concentration S in bioreactor as level of reference substrate concentration S_{ref} by manipulating dilution rate D based on measurement data of S and X. Control constraints are $0 < D < \mu_m, D < \mu, X > 0,\ S > 0$ and $0 < S \leq S_{in}$ for any $t \geq 0$.

5.3 Controller Design

We define $x_1 \equiv S - S_{ref}$ and $x_2 \equiv X$. Because of the uncertainty of specific growth rate, the specific growth rate can be modified as a function including the bounded unknown parameter.

$$\mu x_2 \equiv k_u x_2 + \theta \varphi(x_1, x_2) \tag{5.5}$$

$$\varphi = \frac{k_i \mu_m (x_1 + S_{ref}) x_2}{k_s k_i + k_i (x_1 + S_{ref}) + (x_1 + S_{ref})^2} - k_u x_2 \tag{5.6}$$

where

k_u : unit conversion parameter

$\theta \in [\theta_{min}, \theta_{max}]$: adaptation parameter

With Eq. (5.5) and Eq. (5.6), the system dynamic equation can be written as:

$$\dot{x}_1 = -k k_u x_2 - k\theta\varphi + (S_{in} - x_1 - S_{ref})D - \dot{S}_{ref} \tag{5.7}$$

$$\dot{x}_2 = k_u x_2 + \theta\varphi - D x_2 \tag{5.8}$$

Now, we design controller using adaptive back-stepping method as the following.

Step 1. We define the first tracking error

$$z_1 = x_1 \tag{5.9}$$

whose derivative can be expressed as

$$\dot{z}_1 = -k k_u x_2 - k\theta\varphi + (S_{in} - x_1 - S_{ref})D - \dot{S}_{ref} \tag{5.10}$$

We choose x_2 as virtual input. By putting Eq. (5.10) to be $-c_1 z_1$, $c_1 > 0$ and x_2 can be expressed as

$$x_2 = \frac{c_1 z_1 - k\theta\varphi + (S_{in} - x_1 - S_{ref})D - \dot{S}_{ref}}{kk_u} \tag{5.11}$$

If Eq. (5.11) is replaced by parameter estimate $\hat{\theta}$ of unknown parameter θ, the estimate α_1 of x_2 can be written as

$$\alpha_1 = \frac{c_1 z_1 - k\hat{\theta}\varphi + (S_{in} - x_1 - S_{ref})D - \dot{S}_{ref}}{kk_u} \tag{5.12}$$

We introduce the second error variable as

$$z_2 = x_2 - \alpha_1 \tag{5.13}$$

where α_1 is the stabilizing function for x_2.

$$\dot{z}_1 = \dot{x}_2 = -c_1 z_1 - kk_u z_2 - k\tilde{\theta}\varphi \tag{5.14}$$

Choosing the first Lyapunov function as the following

$$V_1 = \frac{1}{2} z_1^2 + \frac{1}{2\gamma}\tilde{\theta}^2 \tag{5.15}$$

where $\tilde{\theta} = \theta - \hat{\theta}$ is the error of parameter estimation and $\gamma > 0$ is adaptation gain. With Eqs. (5.12) and (5.13), the first derivative of V_1 along the solution of Eq. (5.14) is as follows.

$$\dot{V}_1 = -c_1 z_1^2 - k k_u z_1 z_2 + \tilde{\theta}\left(-k\varphi z_1 - \frac{1}{\gamma}\dot{\hat{\theta}}\right) \tag{5.16}$$

Step 2. According to the computation in Step 1, in case that $\dot{\hat{\theta}} = \gamma \phi z_1$, $\dot{V}_1$ is non-positive in z_1 when $z_2 = 0$. Therefore, we need modify the second Lyapunov function to include the error variable z_2. The modified Lyapunov function is chosen as

$$V_2 = \frac{1}{2} z_2^2 + V_1 \tag{5.17}$$

The derivative of $z_2 = x_2 - \alpha_1$ is

$$\begin{aligned} \dot{z}_2 = & \left(1 + \frac{\hat{\theta}}{k_u}\frac{\partial \varphi}{\partial x_2}\right)\left(k_u x_2 + \theta \varphi - D x_2\right) \\ & - \left(\frac{c_1 - D}{k k_u} - \frac{\hat{\theta}}{k_u}\frac{\partial \varphi}{\partial x_1}\right)\left(-c_1 z_1 - k k_u z_2 - k\tilde{\theta}\varphi\right) + \frac{\varphi}{k_u}\dot{\hat{\theta}} - \frac{\partial \alpha_1}{\partial D}\dot{D} + \frac{1}{k k_u}\ddot{S}_{ref} \end{aligned} \tag{5.18}$$

where

$$\frac{\partial \alpha_1}{\partial D} = \frac{S_{in} - x_1 - S_{ref}}{k k_u} \tag{5.19}$$

$$\frac{\partial \varphi}{\partial x_1} = \frac{k_i \mu_m [k_i k_s - (x_1 + S_{ref})^2] x_2}{[k_s k_i + k_i (x_1 + S_{ref}) + (x_1 + S_{ref})^2]^2} \tag{5.20}$$

$$\frac{\partial \varphi}{\partial x_2} = \frac{k_i \mu_m (x_1 + S_{ref})}{k_s k_i + k_i (x_1 + S_{ref}) + (x_1 + S_{ref})^2} - k_u \tag{5.21}$$

The derivative of V_2 is

$$\dot{V}_2 = -c_1 z_1^2 + \tilde{\theta}\left\{-k\varphi z_1 - \frac{1}{\gamma}\dot{\hat{\theta}} + \left[\left(1 + \frac{\hat{\theta}}{k_u}\frac{\partial\varphi}{\partial x_2}\right)\varphi + \left(\frac{c_1 - D}{kk_u} - \frac{\hat{\theta}}{k_u}\frac{\partial\varphi}{\partial x_1}\right)k\varphi\right]z_2\right\}$$

$$+ z_2\left[-kk_u z_1 + \left(1 + \frac{\hat{\theta}}{k_u} \times \frac{\partial\varphi}{\partial x_2}\right)(k_u x_2 + \hat{\theta}\varphi - Dx_2)\right.$$

$$\left. -\left(\frac{c_1 - D}{kk_u} - \frac{\hat{\theta}}{k_u}\frac{\partial\varphi}{\partial x_1}\right)(-c_1 z_1 - kk_u z_2) + \frac{\varphi}{k_u}\dot{\hat{\theta}} - \frac{\partial\alpha_1}{\partial D}\dot{D} + \frac{1}{kk_u}\ddot{S}_{ref}\right] \qquad (5.22)$$

where the following update law for parameter estimate eliminates $\tilde{\theta}$ -term in Eq. (5.22).

$$\dot{\hat{\theta}} = \gamma\left[k\,\varphi z_1 + \left\{\left(1 + \frac{\hat{\theta}}{k_u}\frac{\partial\varphi}{\partial x_2}\right) + \left(\frac{c_1 - D}{kk_u} - \frac{\hat{\theta}}{k_u}\frac{\partial\varphi}{\partial x_1}\right)k\varphi\right\}z_2\right] \qquad (5.23)$$

The dynamic feedback controller for system stabilization is obtained by letting the last bracket in Eq. (5.22) equal to $-c_2 z_2, c_1 > 0$. After some rearrangement, we have the control dynamics as

$$\dot{D} = \frac{1}{\dfrac{\partial\alpha_1}{\partial D}}\left[-\left(1 + \frac{\hat{\theta}}{k_u}\frac{\partial\varphi}{\partial x_2}\right)x_2 - \frac{1}{kk_u}(kk_u z_2 + c_1 z_1)\right]D$$

$$+ \frac{1}{\dfrac{\partial\alpha_1}{\partial D}}\left[c_2 z_2 - kk_u z_1 + \left(1 + \frac{\hat{\theta}}{k_u}\frac{\partial\varphi}{\partial x_2}\right)(k_u x_2 + \hat{\theta}\varphi)\right.$$

$$\left. + \left(\frac{c_1}{kk_u} - \frac{\hat{\theta}}{k_u}\frac{\partial\varphi}{\partial x_1}\right)(c_1 z_1 + kk_u z_2) + \frac{\varphi}{k_u}\dot{\hat{\theta}} + \frac{1}{kk_u}\ddot{S}_{ref}\right] \qquad (5.24)$$

With Eqs. (5.23) and (5.24), $\dot{V}_2$ is non-positive as follows

$$\dot{V}_2 = -c_1 z_1^2 - c_2 z_2^2 \leq 0 \tag{5.25}$$

By Lasalle-Yoshizawa theorem, the global asymptotic stability is guaranteed at $z_1 = 0$ and $z_2 = 0$. So all of trajectories of the closed loop adaptive system are converged to zero. $\dot{V}_2 = -c_1 z_1^2 - c_2 z_2^2 = 0$ implies that $\lim z_1(t) = 0$ and $\lim z_2(t) = 0$ when $t \to \infty$. Because $z_1 = x_1 = S - S_{ref}$ and $z_2 = x_2 - \alpha_1 = X - \alpha_1$, they imply that $S \to S_{ref}$ and $X \to \alpha_1$.

The closed loop system equations of the process is

$$\dot{z}_1 = -c_1 z_1 - kk_u z_2 - k\tilde{\theta}\varphi \tag{5.26}$$

$$\dot{z}_2 = -c_2 z_2 + kk_u z_1 + \tilde{\theta}\left[\left(1 + \frac{\hat{\theta}}{k_u}\frac{\partial \varphi}{\partial x_2}\right)\varphi + \left(\left(\frac{c_1 - D}{kk_u}\right) - \frac{\hat{\theta}}{k_u}\frac{\partial \varphi}{\partial x_1}\right)k\varphi\right] \tag{5.27}$$

This block diagram of the proposed method is shown in Fig. 39.

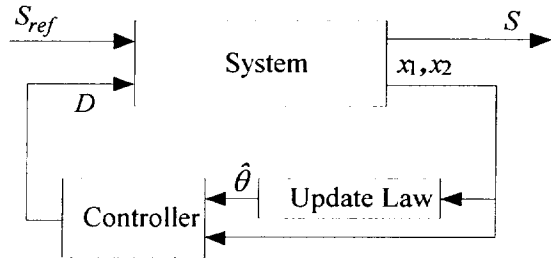

Fig. 39 Block diagram of the proposed method

5.4 Simulation results

To verify the effectiveness of the proposed controller, simulations have been done with the changes of reference substrate and influent substrate. The numerical values used for this simulation follow the work of Simutis et al.[27] and are given as Table 3.

Table 3 The numerical values for simulation

Parameters	Units	Values
Saturation constant k_s	g/*l*	0.1
Maximum specific growth rate μ_m	1/*h*	0.3
Yield coefficient k		2
Inhibition constant k_i	g/*l*	50
Influent substrate concentration S_{in}	g/*l*	20

The unit conversion value is chosen to be k_u=0.275*l*/(*gh*), constants in controller are $c_1 = 7$, $c_2 = 5$, and the adaptation gain is $\gamma = 0.0362$. The initial values used for simulation are $\theta = 1$, $S(1)$=1g/*l*, $X(1)$=0.5g/*l*, and $\hat{\theta}(1) = 1.2$. The first simulation has been done to show the tracking performance of the proposed controller. Reference substrate S_{ref} is assumed to change as a step type as shown in Fig. 40 with the constant influent substrate concentration. The simulation results are shown in Figs. 40-44. The output substrate concentration S tracks reference substrate concentration well as shown in Fig. 40. The variation of the biomass concentration X increases smoothly as shown in Fig. 41. The error estimating parameters $\tilde{\theta}$ converges to zero as shown in Fig. 42. The proposed control input, dilution rate D, and its derivative, dD/dt are shown in Figs. 43 and 44. As shown in Figs. 43 and 44, it is shown that the dilution rate varies in an acceptable range of control constraints mentioned previously.

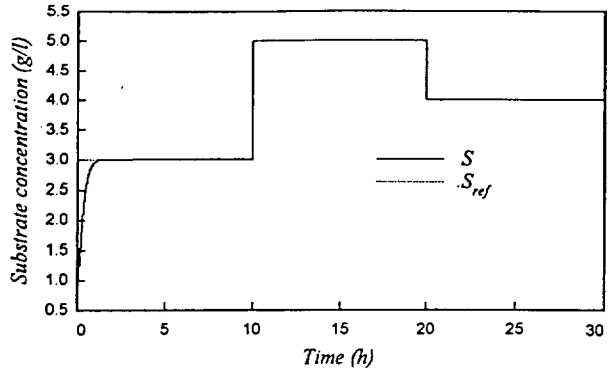

Fig. 40 Output substrate concentration S during the step change of reference substrate concentration S_{ref}

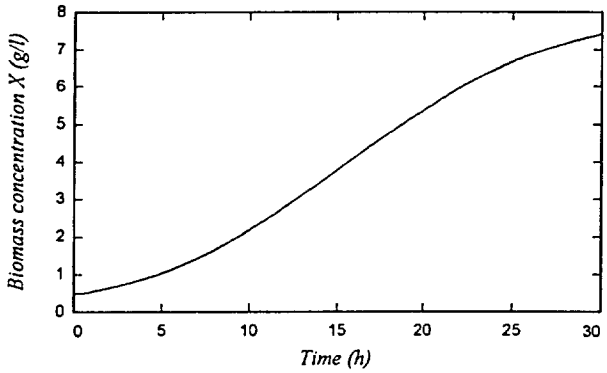

Fig. 41 Biomass concentration X during the step change reference of substrate concentration S_{ref}

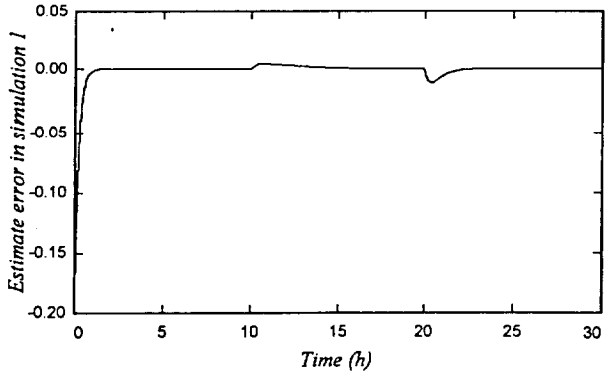

Fig. 42 $\tilde{\theta}$ during the step change of reference substrate concentration S_{ref}

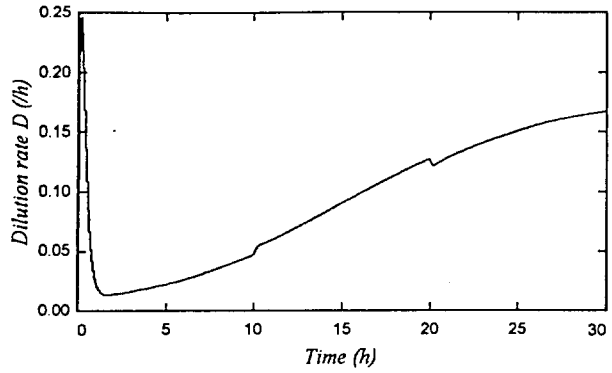

Fig. 43 Dilution rate D (control input) during the step change of reference substrate concentration S_{ref}

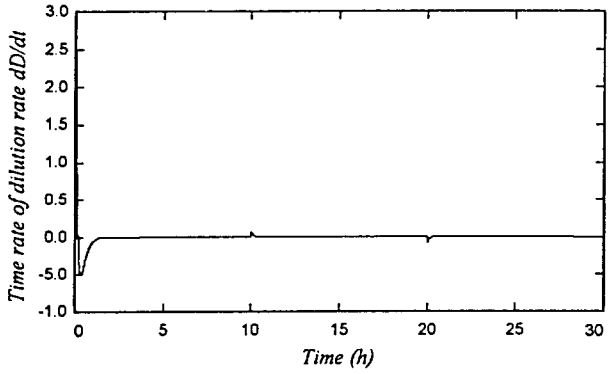

Fig. 44 Time rate of dilution rate dD/dt during the step change of reference substrate concentration S_{ref}

The second simulation has been done with the change of the influent substrate concentration S_{in} with the constant reference substrate. This simulation has been done to know the controlled system performance under disturbance. The change of S_{in} is also to be a step type as 20, 18, and 24 g/l during each 10 hours. The simulation results are shown in Figs. 45-49. Although there are bigger fluctuations at the time with the change of S_{ref} than at the time with the change of S_{in}, the simulation result with the change of the influent substrate concentration S_{in} shows similar results with the changes of reference substrate and also show the good tracking performance to reference well.

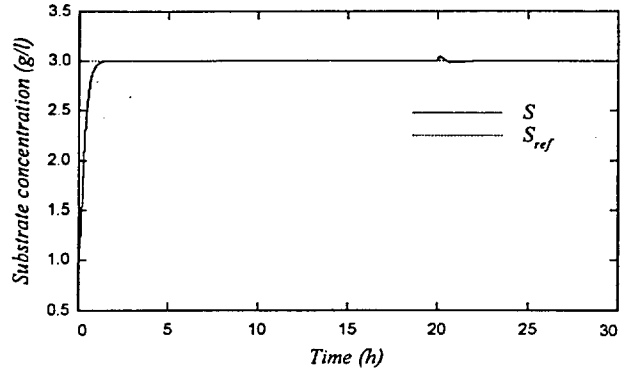

Fig. 45 Output substrate concentration S during the step change of the influent substrate concentration S_{in}

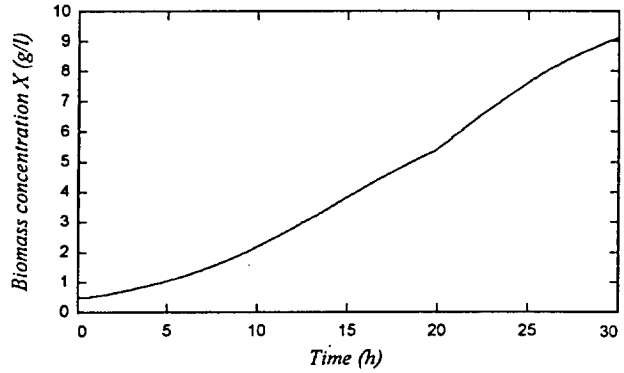

Fig. 46 Biomass concentration X during the step change of the influent substrate concentration S_{in}

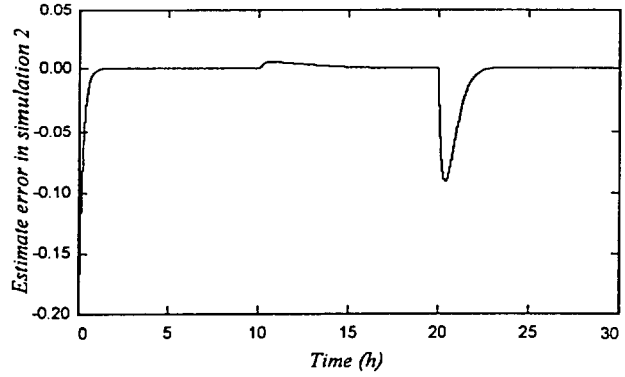

Fig. 47 $\tilde{\theta}$ during the step change of the influent substrate concentration

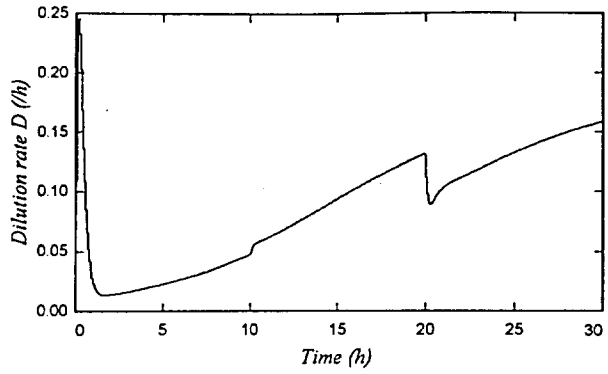

Fig. 48 Dilution rate D (control input) during the step change of the influent substrate concentration S_{in}

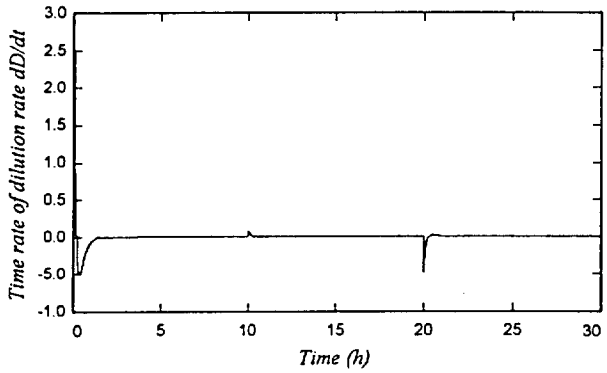

Fig. 49 Time rate of Dilution rate dD/dt during the step change of the influent substrate concentration S_{in}

5.5 Conclusion Remarks

A nonlinear adaptive controller based on back-stepping method has been introduced for a continuous baker's yeast cultivating process in bioreactor. Because of the uncertainty of specific growth rate, the specific growth rate has been modified as a function including the unknown parameter with known bounded values. The simulation results show that the proposed controller can be used for tracking reference substrate concentration with good performance even in

the changes of both reference substrate and influent substrate. The proposed controller rejects the effect of the step change of the influent substrate concentration. Smooth biomass concentration is obtained even in both the change of reference substrate concentration and the variation of influent feed substrate concentration for continuous fermentation processes. The dilution rate increases with constant slope except when reference substrate concentration and influent substrate concentration are changed to track the reference substrate concentration.

VI

Nonlinear Observer for Applications of Fermentation Process in Bioreactor

6.1 Introduction

Fermentation is an important process for cultivating microorganisms. Fermentation can be run as a batch, fed-batch and continuous process. In a continuous system, the substrate is supplied to the bioreactor and extracted from the bioreactor. Fermentation process is so complex, time varying and highly nonlinear. Due to pH, dissolved oxygen, temperature, anti-foam addition, biomass accumulation, production formation and nutrient depletion during fermentation process, the dynamic behavior is significantly changed. So it is difficult to make a model and control for fermentation process exactly. Specially, the exact estimate of the specific growth rate is so uncertain because it depends on parameters such as biomass concentration, substrate concentration, production formulation and temperature, etc. Despite the intensive effort spent in developing new biological sensors in recent years, the sensors are not much exact. To overcome these problems, observers, software sensors, for on-line monitoring biological variables has been developed.

The observer is expected to produce the estimate $\hat{x}(t)$ of the state of $x(t)$ of the original system. One of the reasons of using observer is that full state measurement of a process is generally not available. The construction of observers

is very interesting and there are some available methods have been introduced in literatures. For a linear system, a standard solution is given by the classical Lubenburger observer. For a nonlinear system, the list of references at the end of the paper cover part of recent works done in the area. Gauthier et al.[82] proposed a simple observer for nonlinear system application to bioreactor under general technological assumptions. Farza et al.[79] proposed simple nonlinear observer for estimation in fermentation process. Martinez-Guerra et al.[75] proposed parametric and state estimation using high-gain nonlinear observers applied to bioreactor. Olivera et al.[80] solved the tuning problem of an observer-based algorithm for the on-line estimation of reaction rates in stirred tank bioreactors. Tonambe[83] reduced the estimation of the unknown parameters of a nonlinear system to the estimation of its state variables by a state space immersion using asymptotic high-gain observers. Busawon et al.[76-78] proposed simple high gain observer for a class of nonlinear systems in a special canonical observable form for state and parameter estimation in bioreactor. Among the above papers, the Busawon's high gain observer attained good performance and agreed well with the experimental results. However in some cases, the estimated state of the system is not converged to its real value as fast as required.

This paper proposed a modified observer based on Busawon's high gain observer using an appropriate time dependent function, which can be chosen to make each estimated state converge faster to its real value. The proof is given to prove the stability of the proposed observer using Lyapunov function approach. The fermentation process in stirred tank bioreactor is used for the simulation. Two cases have been done with the original Busawon's observer and the modified observer. The effectiveness of the proposed method is shown through the simulation results applied to bioreactor system.

6.2 High Gain Observer Structure

For general nonlinear system, a high gain observer is used to handle part of the nonlinearity of the system by choosing a sufficiently large value of a given design parameter. This part briefly summaries the high gain observer for a class of nonlinear systems in a special canonical observable form, which is studied by Busawon et al.[78]

Consider single-output system as follows:

$$\dot{z} = F(s,z)\,z + G(u,s,z) \tag{6.1}$$

$$y = C\,z \tag{6.2}$$

where

$$F(s,z) = \begin{bmatrix} 0 & f_1(s,z) & 0 & \cdots & 0 \\ 0 & 0 & f_2(s,z) & \cdots & 0 \\ \vdots & \vdots & \vdots & \ddots & \vdots \\ 0 & 0 & 0 & \cdots & f_{n-1}(s,z) \\ 0 & 0 & 0 & \cdots & 0 \end{bmatrix} \tag{6.3}$$

$$G(u,s,z) = \begin{bmatrix} g_1(u,s,z_1) \\ \vdots \\ g_n(u,s,z_1,z_2,\cdots,z_n) \end{bmatrix} \tag{6.4}$$

$$C = \begin{bmatrix} 1 & 0 & \cdots & 0 \end{bmatrix} \tag{6.5}$$

$z = (z_1, z_{2,\cdots,} z_n) \in R^n$, $u \in R^m$, $y \in R$ and s is a known function, f_i are class C^1 that the first derivatives are continuous with respect to their arguments.

Let $N(s,\xi,t)$ be observability matrix for system Eqs. (6.1)-(6.5) as follows

$$N(s,\xi,t) = diag\left[1, f_1(s,\xi), f_1(s,\xi)f_2(s,\xi), \cdots, f_1(s,\xi)f_2(s,\xi)\cdots f_{n-1}(s,\xi)\right] \tag{6.6}$$

Consider the following algebraic Lyapunov equation

$$\frac{dS_\lambda}{dt} = \lambda S_\lambda + A^T S_\lambda + S_\lambda A - C^T C = 0 \tag{6.7}$$

where S_λ is the symmetric positive definite matrix, λ is a positive number and matrix A is of the form:

$$A = \begin{bmatrix} 0 & 1 & \cdots & 0 \\ \vdots & \ddots & \ddots & \vdots \\ 0 & 0 & \cdots & 1 \\ 0 & 0 & \cdots & 0 \end{bmatrix} \tag{6.8}$$

We assume the followings:

(A1) There exists a subset $U \subset L^\infty(R^+, R^m)$ and two compact sets $K_1 \subset K_2$ such that every trajectory $z(t)$ associated to any $u \in U$ and issued from K_1 to K_2.

(A2) $s(t)$ is known and bounded in class C^1 and $\dot{s}(t)$ is also bounded.

(A3) $\exists \alpha_1 > 0, \forall u \in R^m, \forall z \in R^n, \forall t \geq 0 : |f_i(s(t), z)| > \alpha_1$

(A4) $\exists \alpha_2 > 0, \forall u \in R^m, \forall z \in R^n, \forall t \geq 0 : |g_i(\mathrm{u}, s(t), z)| > \alpha_2$ for $i = 1, \cdots, n$.

(A5) $\exists \beta, \gamma \geq 0; \forall u \in R^m, \forall z \in R^n; \forall t \geq 0$

$$\left\| \frac{\partial f_j(s(t), z)}{\partial z} \right\| \leq \beta, \quad \left\| \frac{\partial g_i(u(t), s(t), z)}{\partial z} \right\| \leq \gamma$$

for $j = 1, \cdots, n\text{-}1$ and $i = 1, \cdots, n$.

(A6) $N(s, \xi, t)$ is full rank for all $t \geq 0$ and its time derivative is bounded.

Theorem 1[78]: Assume that the system (6.1) satisfies Assumptions (A1)-(A6). Then, there exists $\lambda > 0$ such that the following equation is an exponential observer for the system (6.1):

$$\dot{\hat{z}} = F(s,\hat{z})\hat{z} + G(u,s,\hat{z}) - N^{-1}(s,\hat{z},t)S_{\lambda}^{-1}C^{T}(C\,\hat{z} - y) \tag{6.9}$$

6.3 Modified Observer

This section introduces a modified observer based on the above Busawon's high gain observer using an appropriate time dependent function $H(t)$, which can be chosen to make each estimated state converge faster to its real value.

$$H(t) = diag\left[1, h_1(t), h_2(t), \cdots, h_{n-1}(t)\right] \tag{6.10}$$

Now, let $M(s,\xi,t)$ be observability matrix for system Eqs. (6.1)-(6.5) as follows:

$$M(s,\xi,t) = diag\left[1, f_1(s,\xi), \frac{f_1(s,\xi)f_2(s,\xi)}{h_1(t)}, \cdots, \frac{f_1(s,\xi)f_2(s,\xi)\cdots f_{n-1}(s,\xi)}{h_1(t)h_2(t)\cdots h_{n-2}(t)}\right] \tag{6.11}$$

We assume the followings:

(A7) $H(t)$ is bounded function and $\text{rank}(H(t)) = n$.

(A8) $M(s,\xi,t)$ is full rank for all $t \geq 0$ and its time derivative is bounded.

The proposed modified observer can be cited in the following theorem 2.

Theorem 2: Assume that the system (6.1) satisfies Assumptions (A1)-(A5) and (A7)-(A8). Then, there exists $\lambda > 0$ such that the following equation is an exponential observer for the system (6.1):

$$\dot{\hat{z}} = F(s,\hat{z})\hat{z} + G(u,s,\hat{z}) - H(t)M^{-1}(s,\hat{z},t)S_{\lambda}^{-1}C^{T}(C\,\hat{z} - y) \tag{6.12}$$

Proof of theorem 2

For the sake of simplicity, note that $F \equiv F(s,z)$, $\hat{F} \equiv F(s,\hat{z})$, $G \equiv G(u,s,z)$, $\hat{G} \equiv G(u,s,\hat{z})$, $H \equiv H(t)$ and $\hat{M} \equiv M(s,\hat{z},t)$.

Define the observer error, $\varepsilon = \hat{z} - z$. Its first derivative yields

$$\begin{aligned}\dot{\varepsilon} &= \dot{\hat{z}} - \dot{z} \\ &= (\hat{F} - H\hat{M}^{-1}S_{\lambda}^{-1}C^{T}C)\varepsilon + (\hat{F} - F)z + (\hat{G} - G)\end{aligned} \tag{6.13}$$

Now define a new variable

$$\bar{\varepsilon} = \hat{M}\Delta_{\lambda}\varepsilon \;\rightarrow\; \varepsilon = \Delta_{\lambda}^{-1}\hat{M}^{-1}\bar{\varepsilon} \tag{6.14}$$

where

$$\Delta_{\lambda} = \mathrm{diag}\left[1, \frac{1}{\lambda}, \frac{1}{\lambda^{2}}, \cdots, \frac{1}{\lambda^{n-1}}\right] \tag{6.15}$$

then we have

$$\dot{\bar{\varepsilon}} = \dot{\hat{M}}\Delta_{\lambda}\varepsilon + \hat{M}\Delta_{\lambda}\dot{\varepsilon}$$

Using relation shown in part A of Appendix 2, we can derive the following

$$\dot{\bar{\varepsilon}} = \dot{\hat{M}}\hat{M}^{-1}\bar{\varepsilon} + \lambda(A - HS_1^{-1}C^TC)\bar{\varepsilon} + \hat{M}\Delta_\lambda(\hat{F} - F)z + \hat{M}\Delta_\lambda(\hat{G} - G) \tag{6.16}$$

The Lyapunov function is chosen as follows

$$V = \bar{\varepsilon}^T S_1 \bar{\varepsilon} = \|\bar{\varepsilon}\|_{S_1}^2 \geq 0 \tag{6.17}$$

Using Eqs. (6.14)-(6.16) and the relation in part B of Appendix 2, the first derivative of Lyapunov function can be written as

$$\begin{aligned}
\dot{V} &= 2\bar{\varepsilon}^T S_1 \dot{\bar{\varepsilon}} \\
&= 2\bar{\varepsilon}^T S_1 \dot{\hat{M}}\hat{M}^{-1}\bar{\varepsilon} - \lambda V \\
&\quad - \lambda\bar{\varepsilon}^T C^T C\bar{\varepsilon} - 2\lambda\,\bar{\varepsilon}^T S_1 (H - I)\, S_1^{-1} C^T C\bar{\varepsilon} \\
&\quad + 2\bar{\varepsilon}^T S_1 \hat{M}\Delta_\lambda(\hat{F} - F)z + 2\bar{\varepsilon}^T S_1 \hat{M}\Delta_\lambda(\hat{G} - G) \\
\dot{V} &\leq -\lambda V + 2\left\|\dot{\hat{M}}\hat{M}^{-1}\right\| \|S_1\bar{\varepsilon}\| \|\bar{\varepsilon}\| \\
&\quad - \lambda\|C\varepsilon\|^2 - 2\lambda\|S_1\bar{\varepsilon}\|\,\|\bar{\varepsilon}\|\left\|(H - I)S_1^{-1}C^TC\right\| \\
&\quad + 2\|S_1\bar{\varepsilon}\|\left\|\hat{M}\right\|\left\|\Delta_\lambda(\hat{F} - F)z\right\| + 2\|S_1\bar{\varepsilon}\|\left\|\hat{M}\right\|\left\|\Delta_\lambda(\hat{G} - G)\right\|
\end{aligned} \tag{6.18}$$

Using Assumption (A5), the boundedness of the state and the triangular structure of G and f_i, with some positive constants γ_1, γ_2, we obtain[78]

$$\begin{aligned}
\left\|\Delta_\lambda(\hat{F} - F)z\right\| &\leq \gamma_1\|\Delta_\lambda\varepsilon\| = \gamma_1\left\|\hat{M}^{-1}\bar{\varepsilon}\right\| \leq \gamma_1\left\|\hat{M}^{-1}\right\|\|\bar{\varepsilon}\| \\
\left\|\Delta_\lambda(\hat{G} - G)\right\| &\leq \gamma_2\|\Delta_\lambda\varepsilon\| = \gamma_2\left\|\hat{M}^{-1}\bar{\varepsilon}\right\| \leq \gamma_2\left\|\hat{M}^{-1}\right\|\|\bar{\varepsilon}\|
\end{aligned}$$

Define $\eta_1 \equiv \left\| \dot{\hat{M}}\, \hat{M}^{-1} \right\|$, $\eta_2 \equiv \left\| (H - I)\, S_1^{-1} C^T C \right\|$,

$$\left\| S_1 \bar{\varepsilon} \right\| \left\| \bar{\varepsilon} \right\| \equiv \sigma V = \sigma \bar{\varepsilon}^T S_1 \bar{\varepsilon}\,, \quad \rho \equiv 2\eta_1 + 2_1\gamma_1 + 2\gamma_2$$

Then we can rewrite (6.18) as follows

$$\dot{V} \le -\lambda V + 2\eta_1 \left\| S_1 \bar{\varepsilon} \right\| \left\| \bar{\varepsilon} \right\| + 2\gamma_1 \left\| S_1 \bar{\varepsilon} \right\| \left\| \bar{\varepsilon} \right\|$$

$$+ 2\gamma_2 \left\| S_1 \bar{\varepsilon} \right\| \left\| \bar{\varepsilon} \right\| - 2\lambda \left\| S_1 \bar{\varepsilon} \right\| \left\| \bar{\varepsilon} \right\| \eta_2$$

$$\dot{V} \le -[\lambda(1 + 2\eta_2\sigma) - \rho\sigma] V \tag{6.19}$$

If λ is chosen so as to satisfy $\lambda \ge (\rho\sigma)/(1 + 2\eta_2\sigma)$, $\dot{V}$ achieves negative. Hence, $\bar{\varepsilon} \to 0$, $\varepsilon = \Delta_\lambda^{-1} \hat{M}^{-1} \bar{\varepsilon} \to 0$ when $t \to \infty$. ■

When the matrix $H(t)$ in (6.10) is chosen as an identity matrix, the proposed observer is the high-gain nonlinear observer which has been studied in the works of Busawon et al.[78]. The first element of $H(t)$ is 1 corresponding to the measured state of system. Another element of $H(t)$ can be chosen under the Assumption (A7) to make the estimated state converge faster to its real value.

6.4 Application to Bioreactor

In this section , the system dynamic equations on the substrate and the biomass in bioreactor are given in section 5.2. The observer of the system dynamic equations is designed.

We consider two cases: 1) measure substrate concentration S and then estimate biomass concentration X using Haldane's specific growth rate and 2) measure

biomass concentration X and then estimate the specific growth rate μ without any assumption on its model.

* *Case 1: Estimation of X from the measurement of S when μ satisfies Haldane's law.*

The system can be rewritten in the following form

$$\begin{bmatrix} \dot{S} \\ \dot{X} \end{bmatrix} = \begin{bmatrix} 0 & -k\mu(S) \\ 0 & 0 \end{bmatrix} \begin{bmatrix} S \\ X \end{bmatrix} + \begin{bmatrix} D(S_{in} - S) \\ \mu(S)X - DX \end{bmatrix} \tag{6.20}$$

$$y = \begin{bmatrix} 1 & 0 \end{bmatrix} \begin{bmatrix} S \\ X \end{bmatrix} \tag{6.21}$$

Apply the proposed observer (6.12) with

$$\hat{z} = [\hat{S} \quad \hat{X}]^T$$

$$F(s,\hat{z}) = \begin{bmatrix} 0 & f_1(s,\xi) \\ 0 & 0 \end{bmatrix} = \begin{bmatrix} 0 & -k\mu(\hat{S}) \\ 0 & 0 \end{bmatrix}$$

$$\mu(\hat{S}) = \frac{k_i \mu_m \hat{S}}{k_s k_i + k_i \hat{S} + \hat{S}^2}$$

$$G(u,s,\hat{z}) = \begin{bmatrix} D(S_{in} - \hat{S}) \\ \mu(\hat{S})\hat{X} - D\hat{X} \end{bmatrix}$$

$$H(t) = \begin{bmatrix} 1 & 0 \\ 0 & 1 - e^{-t} \end{bmatrix}$$

$$M^{-1}(s,\hat{z},t) = \begin{bmatrix} 1 & 0 \\ 0 & \dfrac{1}{f_1(s,\hat{z})} \end{bmatrix} = \begin{bmatrix} 1 & 0 \\ 0 & -\dfrac{1}{k\mu(\hat{S})} \end{bmatrix}$$

$$S^{-1}{}_{\lambda} = \begin{bmatrix} 2\lambda & \lambda^2 \\ \lambda^2 & \lambda^3 \end{bmatrix}$$

$$C = \begin{bmatrix} 1 & 0 \end{bmatrix}$$

$$\hat{z} - z = \begin{bmatrix} \hat{S} - S & \hat{X} - X \end{bmatrix}^T$$

The proposed observer is as follows

$$\begin{cases} \dot{\hat{S}} = -k\mu(S)\hat{X} + (S_{in} - \hat{S})D - 2\lambda(\hat{S} - S) \\ \dot{\hat{X}} = \mu(\hat{S})\hat{X} - \hat{X}D + (1 - e^{-t})\dfrac{\lambda^2}{k\mu(\hat{S})}(\hat{S} - S) \end{cases} \tag{6.22}$$

* *Case 2: Estimation of μ from the measurement of X without any assumption on the model of μ*

In this case, no information on μ is available, we assume instead that μ satisfies $\dot{\mu} = \phi(t)$ with unknown bounded function $\phi(t)$. The system can be rewritten in the following form

$$\begin{bmatrix} \dot{X} \\ \dot{\mu} \end{bmatrix} = \begin{bmatrix} 0 & X \\ 0 & 0 \end{bmatrix} \begin{bmatrix} X \\ \mu \end{bmatrix} + \begin{bmatrix} -XD \\ \phi \end{bmatrix} \tag{6.23}$$

$$y = \begin{bmatrix} 1 & 0 \end{bmatrix} \begin{bmatrix} X \\ \mu \end{bmatrix} \tag{6.24}$$

Apply the proposed observer (6.12) to the system with

$$\hat{z} = [\hat{X} \quad \hat{\mu}]^T$$

$$F(s, \hat{z}) = \begin{bmatrix} 0 & f_1(\mathrm{s}, \xi) \\ 0 & 0 \end{bmatrix} = \begin{bmatrix} 0 & \hat{X} \\ 0 & 0 \end{bmatrix}$$

$$G(u,s,\hat{z}) = \begin{bmatrix} -\hat{X}D \\ \hat{\phi} \end{bmatrix}$$

$$H(t) = \begin{bmatrix} 1 & 0 \\ 0 & 1-e^{-t} \end{bmatrix}$$

$$M^{-1}(s,\hat{z},t) = \begin{bmatrix} 1 & 0 \\ 0 & \dfrac{1}{f_1(s,\hat{z})} \end{bmatrix} = \begin{bmatrix} 1 & 0 \\ 0 & \dfrac{1}{\hat{X}} \end{bmatrix}$$

$$S^{-1}{}_{\lambda} = \begin{bmatrix} 2\lambda & \lambda^2 \\ \lambda^2 & \lambda^3 \end{bmatrix}$$

$$C = \begin{bmatrix} 1 & 0 \end{bmatrix}$$

$$\varepsilon = \hat{z} - z = \begin{bmatrix} \hat{X} - X & \hat{\mu} - \mu \end{bmatrix}^T$$

which yields

$$\begin{cases} \dot{\hat{X}} = \hat{\mu}\hat{X} - \hat{X}D - 2\lambda(\hat{X} - X) \\ \dot{\hat{\mu}} = -(1-e^{-t})\lambda^2 \dfrac{\hat{X} - X}{\hat{X}} \end{cases} \tag{6.25}$$

The time dependent function is chosen as $h_1(t) = 1 - e^{-t}$, this function is stable and converges to unit when $t \to \infty$. Hence it satisfies Assumption (A7).

Remark: In chapter 5, the controller is designed used for keeping the substrate concentration in bioreactor for smoothly increasing cultivation of microorganism. However, the observer design is needed to practically implement exact control and know the internal state of the system. In this chapter, the two observer design methods are proposed for estimating the states of bioreactor system, states X and μ mentioned as above. Generally, the observer is used to control the system for estimating the states and designing more exact control system. That is, because of

using all states by introducing them to the controller designed in chapter 5 using the states obtained by the observer, exact control can be implemented. Finally, biomass concentration X can be obtained by the counting algorithm using digital image processing in chapter 2-4.

6.5 Simulation Results

To verify the effectiveness of the proposed observer, simulations have been done with Busawon's observer and the proposed modified observer. In Busawon observer, $H(t) = diag([1,1])$ and in the proposed modified observer, $H(t) = diag([1, 1-e^{-t}])$. The noise of zero mean and standard deviation of 10% is used in this simulation.

The first simulation is done with estimation of X from the measurement of S when μ satisfies Haldane's law. Parameter λ is chosen as 6. Simulation results are given in Figs. 50-53. Fig. 50 shows reference substrate concentration S_{ref}, output substrate concentration S and estimated substrate concentration $\hat{S}$ by proposed method and Busawon method when reference substrate S_{ref} is assumed to be changed as a step type with the constant influent substrate concentration. Because we measure S, the values of $\hat{S}$ can be estimated using Busawon's and the proposed observer's results are not far from those real values. Fig. 51 shows output biomass concentration X and those estimated values $\hat{X}$ using both observers. The proposed observer estimates output substrate concentration S and biomass concentration X faster than Busawon's observer as shown in Figs. 50 and 51. The errors of estimation are given in Figs. 52 and 53. Both figures show that the proposed observer has better performance comparing to Busawon's observer. When the time is large enough, both observers are identical because we choose $h_1(t) = 1 - e^{-t}$ which converges to unit when $t \to \infty$.

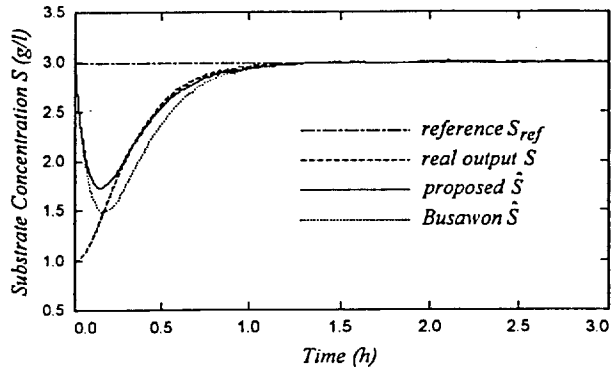

Fig. 50 Substrate concentrations: reference, estimations and output during the step change of biomass substrate concentration

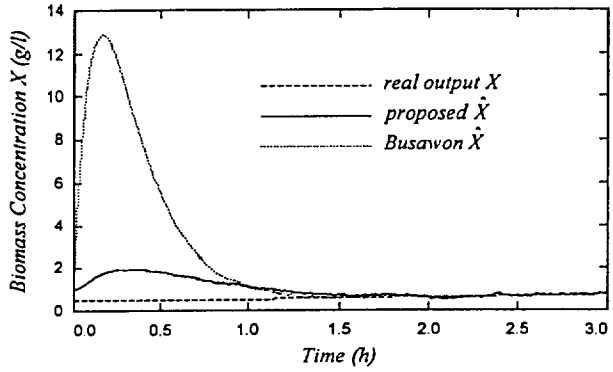

Fig. 51 Biomass concentrations: estimations and output during the step change of biomass substrate concentration

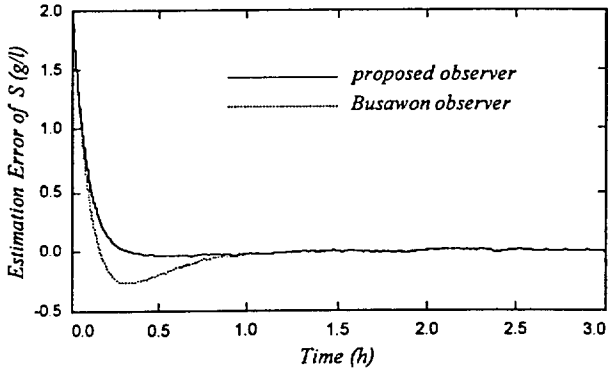

Fig. 52 Errors of estimated substrate concentration

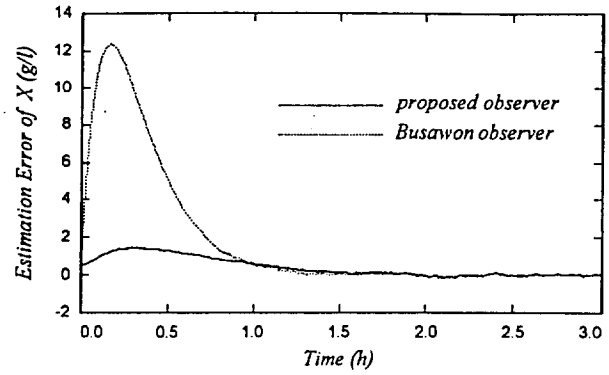

Fig. 53 Errors of estimated biomass concentration

The second simulation is done with estimation of μ from the measurement of X without any assumption on the model of μ. Parameter λ is chosen as 2.68. Simulation results are given in Figs. 54-57. Fig. 54 shows the biomass concentrations and their errors are given in Fig. 56. The specific growth rates of the controlled process are given in Fig. 55 and their errors are given in Fig. 57. The bigger value of λ is chosen, the faster the estimation value converges to its real value. Of course, there is the bigger estimation error. From these figures, we can conclude that the proposed observer has a better performance comparing to the original Busawon's observer.

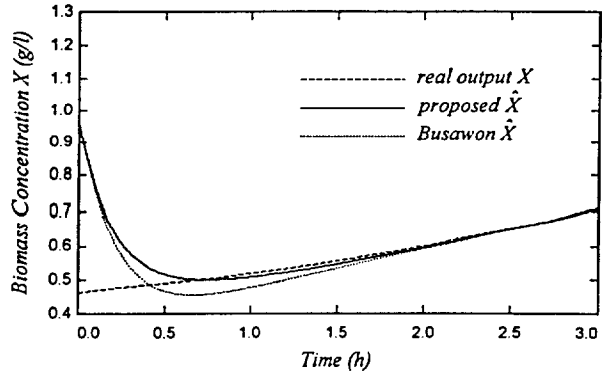

Fig. 54 Biomass concentration

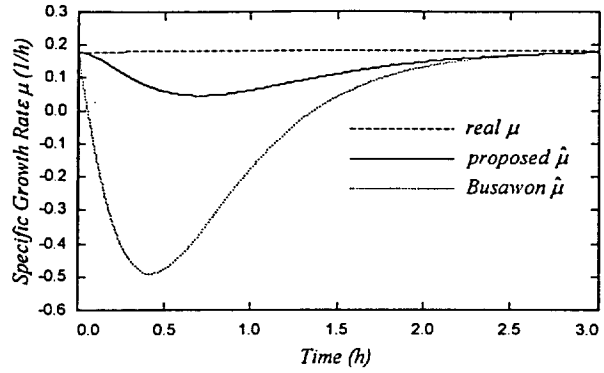

Fig. 55 Specific growth rates: real value, estimated values with proposed and Busawon's observer

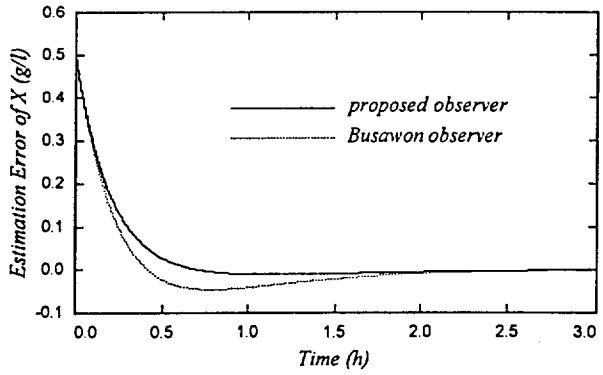

Fig. 56 Errors of estimated biomass concentration

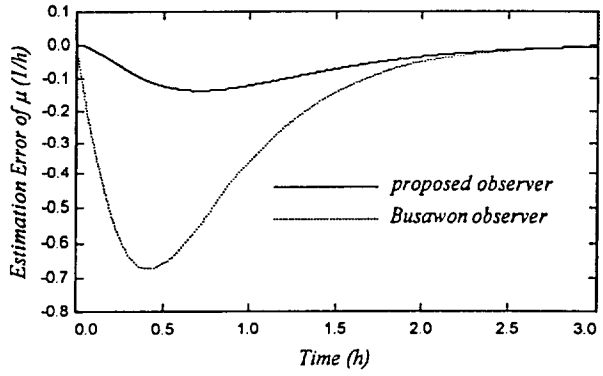

Fig. 57 Errors of estimated specific growth rate

6.6 Conclusion Remarks

A modified nonlinear observer based on Busawon's observer is introduced. By using appropriate time dependent bounded function, the modified observer shows faster convergence to its real value than Busawon's observer. The proof of the stability of the modified observer using Lyapunov function approach is given. The modified observer is applied for estimating output substrate concentration and biomass concentration of a continuous baker's yeast cultivating process in stirred tank bioreactor. In the case of using no model of specific growth rate, we can also use the proposed observer to estimate the specific growth rate using only measuring the biomass concentration. The effectiveness of the modified observer is shown through the simulation. The simulation results show that the proposed observer has good performance with smaller error and faster estimation than Busawon's observer.

VII

Conclusions

This paper proposes the algorithms counting microorganism and controlling cultivating process in bioreactor using image processing method.

Microscopic images of cultivated microorganism in bioreactor are colorless. They also have a lot of noises, overlapped images and un-uniform gray values. The proposed algorithms to effectively count microorganism in bioreactor are proposed.

Nonlinear adaptive controller is proposed to track the reference substrate concentration for smoothly increasing biomass concentration in bioreactor. The proposed observer based on Busawon's observer is introduced to estimate the system parameters in bioreactor.

The effectiveness of the proposed methods is shown through the results of simulations and experiments.

7.1 Results

The results in the thesis can be summarized as follows

- For counting non-overlapped image, the following two methods are proposed.
  - Using area filter and morphological filters as cleaning, filling and opening.
  - Using two-dimensional cubic surface fitting method and minimum square error method to eliminate and reconstruct background.

The second method is more effective than the first method for counting the images contaminated with severe noises. However, both methods are not effective for counting overlapped image.

- For counting overlapped image, we propose the hybrid algorithm including Otsu's optimal thesholding method in 2×2 block, elongating marker algorithm and conventional watershed algorithm. This method is effective for counting cells in all microscopic noisy and overlapped images.
- Nonlinear adaptive controller based on back-stepping method can track the reference substrate concentration by increasing the dilution rate as a control input with constant slope even in the step change of reference concentration and influent substrate concentration. Smooth increasing biomass concentration can be obtained.
- The proposed observer have good performance of converging faster to its real value than Busawon's observer both in estimating biomass concentration from the measurement of the substrate concentration and in estimating specific growth rate from the measurement of biomass concentration.

7.2 Future Work

- Carry out the reliability test with many experiments to verify the accuracy of the count obtained by the proposed method.
- The proposed counting algorithm in the thesis still segments some overlapped images and over-segmentation. Develop new algorithm to solve these problems.
- The effectiveness of controller and observer proposed in thesis is shown through the results of the experiment.

References

[1] Hannah, I., D. Patel and R. Davies, "The Use of Variance and Entropic Thresholding for Image Segmentation", Pattern Recognition, Vol. 28, pp. 1135-1143.

[2] Morii, F., "An Image Thresholding Method Using A Minimum Weighted Squared-distortion Criterion", Pattern Recognition, Vol. 28, 1063-1071, 1995.

[3] Chowdhury, M. H. and W. D. Little, "Image Thresholding Techniques", IEEE Pacific Rim Conference on Communications, Computers, and Signal Processing, pp. 585-589, 1995.

[4] Cheriet, M., J. N. Said, and C. Y. Suen, "A Recursive Thresholding Technique for Image Segmentation", Institute of Electrical and Electronics Engineers(IEEE) Transaction on Image Processing, Vol. 7, No. 6, pp. 918-921, 1998.

[5] Jianzhuang, L. and L. Wenqing and T. Yupeng, "Automatic Thresholding of Gray-level Pictures Using Two-dimensional Ostu Method", International Conference on Circuits and Systems, Vol. 1, pp. 325-327, 1991.

[6] Otsu, N., "A Threshold Selection Method from Gray-level Histograms", IEEE Trans. Syst. Man Cybern. 9, pp. 62-66, 1979.

[7] Pitas, I., *Digital Image Processing Algorithms*, Prentice Hall, N.Y., pp. 254-281, 1993.

[8] Thomas, C. R. and O. C. Paul, "Application of Image Analysis in Cell Technology", Curr. Opin. Biotech., Vol. 7, pp. 35-45, 1993.

[9] Zalewski, K. and E. E. Bildanalyse, "System Zur On-line Charakterisierung von Hefesuspensione", Master of Diploma, TU-Berlin, VDI-Verlag GmbH, 1995.

[10] Bloem, J., M. Veninga and J. Shepher, "Fully Automatic Determination of Soil Bacterium Numbers, Cell Volumes, and Frequencies of Dividing Cells by Confocal Laser Scanning Microscopy and Image Analysis", Appl. Environ. Microbiol, Vol. 61, pp. 926-936, 1995.

[11] Castleman, K. R, *Digital Image Processing*, Prentice Hall, Englewood Cliffs, New Jersey, pp. 123-645, 1996.

[12] Pons, M. N., H. Vivier, J. F. Remy and J. A. Dodds, "Morphological Characterization of Yeast by Image Analysis", Biotech. Bioeng., Vol. 42, pp. 1352-1359, 1993.

[13] Sonka, M., V. Hlavac and R. Boyle, *Image, Processing, Analysis and Machine Vision*, Brooks/Cole Publishing Company. CA., pp. 123-133, 1999.

[14] Suhr, H. and G. Wehnert, "In Situ Microscopy for On-line Characterization of Cell-populations in Bioreactors, Including Cell-concentration Measurements by Depth from Focus", Biotech. Bioeng., Vol. 47, pp. 106-116, 1995.

[15] Bittner, C., G. Wehnert, and T. Scheper, "In-situ Microscopy for On-line Determination of Biomass", Biotechnology and Bioengineering, Vol. 60, No. 1, Oct. 5, 1998.

[16] Reichl, U., T. Buschulte, and E. Gilles, "Study of the Early Growth and Branching of Streptomyces Tendae by Means of an Image Processing System", Journal of Microscopy, Vol. 58, pp. 55-62, 1990.

[17] Salembia, P. and J. Serra, "Morphological Multiscale Segment- ation of Images", The International Society for Optical Engineering(SPIE) Visual Communication Image Processing, 92 Boston , MA, Vol. 1818, No. 2, pp. 621-631, 1992.

[18] Lee, M. S. and J. H. Park, "Isolation of Ammonia-oxidizing Bacteria and Their Characteristic", Journal of the Korean Fisheries Society, Vol. 31, pp. 769-766, 1998.

[19] Beucher, S. and C. Lantuejoul, "Use of Watershed in Contour detection", International Workshop on Image Processing: Real-Time Edge and Motion Detection/Estimation, Rennes, France, pp. 17-21, 1979.

[20] Vincent, L. and P. Soille, "Watershed in Digital Spaces: An Efficient Algorithm Based on Immersion Simulations", IEEE Transactions on Pattern Analysis and Machine Intelligence, Vol. 13, No. 6, pp. 583-598, 1993.

[22] Choi, M. K., H. Y. Han, Y. H. Jung and K. H. Min, "A Composition of Nitrite Production by Ammonium Oxidizing Bacteria Xanthomonas Maltophila SU6 and Achromobacter sp.", 12A. Kor. J. Microbiol, Vol. 32, No. 6, pp, 517-524, 1994.

[23] Sireacki, M. E., S. E. Reichenbach, K. L.Webb, "Evaluation of Automated Threshold Selection Methods for Accurated SizigMicroscopic Fluorescent Cells by Image Analysis", Applied & Environmeta MicroBiology, 1985.

[24] Viles, C. L., M. E. Sieracki, "Measurement of Mirine Pikoplankton Cell size by Using a cooled, charged-coupled Device Camera with image-Analyzed Fluorescene Microscopy", Applied & Environmetal MicroBiology, pp. 584-592, 1992.

[25] Tham, H. J., M. A. Hussain, K. B. Ramachandran, "Variable Structure Control for a Continuous Bioreactor", Proceeding to TENCON2000, IEEE Region 10 Conference, Vol. 1, pp. I-433-I436, 2000.

[26] Zlateva, P., "Sliding-mode Control of Fermentation Process", Bioprocess Engineering 16, Springer-Verlag Wienna/New York, pp. 383-387, 1997.

[27] Simutis, R., R. Oliveire, M. Manikowski, et. al, "How to Increase of Performance of Models for Proces Optimization and Control", Journal of Biotechnology, Vol. 59, pp. 73-89, 1997.

[28] Levine, W., *The Control Handbook, Vol. II,* CRC Press and IEEE Press, pp. 980-993, 1996.

[29] Krstic, M., I. Kanellakopoulos and P. Kokotovic, *Nonlinear and Adaptive Control Design*, John Wiley & Sons, Inc., pp. 92-183, 1995.

[30] Roux, G., B. Dahhou, "Adaptive Non-Linear Control of a Real-life Fermentation Process", Control Application, Proceedings of the Third IEEE Conference on, pp. 909-913, 1994.

[31] Schneider, R., N. A. Jale, A. Munack and J. R. Leigh, "Adaptive Prediction Control for the Fed-batch Fermentation Pocess", Control, International IEEE Conference on, Vol. 1, pp. 249-254, 1994.

[32] Chen, L., G. Bastin, V. V. Breusegem, "Adaptive Nonlinear Regulation of Fed-Batch Biological Reactor: An Industrial Application", Decision and Control, Proceedings of the 30th IEEE Conference on, pp. 2130-2134, 1991.

[33] Maher, M., B. Dahou and F. Y. Zeng, "Adaptive Filtering and Estimation of Nonlinear Biological System", Systems, Man and Cybernetics, Vol. 4, pp. 235-240, 1993.

[34] Nguyen, T. T., H. R. Yoo, Y.W. Rho and S. B. Kim, "Speed Control of PIG Using Bypass Flow in Natural Gas Pipeline", Proceeding of the 6th IEEE International Symposium on Industrial Electronics(ISIE' 2000), Vol. 2, pp Pusan, Korea, 863-868, 2001.

[35] 김상봉, 하주식, *메카니컬 시스템제어*, 한미출판사, 1992.

[36] 김상봉, 하주식, *기초시스템이론*, 한미출판사, 1990.

[37] Sastry, S., *Nonlinear System*, Springer-Velag, New York, 1999.

[38] Isidori, A., *Nonlinear Control System*, Springer-Velag, London, 1994.

[39] Khail, H. K., *Nonlinear System*, Prentice Hall, Upper Saddle River, NJ, 1996.

[40] Dawson, D. M., J. Hu and T. C. Burg, *Nonlinear Control of Electronic Machinery*, Marcel Dekker, Inc., NY, 1998.

[41] Ukin, V., J. Guldner and J. Shi, *Sliding Mode Control in Electromechanical Systems*, Taylor & Francis Ltd. London, 1999.

[42] Crane, R., *A Simplified Approach to Image Processing*, Prentice Hall, Upper Saddle River, NJ, 1997.

[43] Gonzalez, R. C. and R. E. Woods, *Digital Image Processing*, Addison-Wesley Publishing Company, NY, 1993.

[44] Burdick, H., *Digital Imaging Theory and Applications*, McGraw-Hill, 1997.

[45] Gose, E. R. Johnsonbaugh and S. Jost, *Pattern Recognitition and Image Analysis*, Prentice Hall, 1996.

[46] MacDonald, L. W. and M. R. Luo, *Colour Imaging Vision and Technology*, John Wiley & Sons Ltd., 1999.

[47] 구윤모, 서진호, 장용근, 박태호 공역, *생물공정공학*, 교보문고, 1997.

[48] Barnard, E. A., A. C. Bloomer, K. E. Davies, S. P. Hunt, R. J. Keynes, T. H. Rabbits, P. H. Rubery, M. F. Tuite, C. Watts, Sir D. J. Weatherall and R. A. H. White, "The Encyclopedia of Molecular Biology", Blackwell Science, Germany, pp. 568.

[49] Purves, W. K., G. H. Orians, H. C. Heller and D. Sadava, "Life The Science of Biology", Sinauer Associates, INC, pp. 205-206.

[50] Ng, W. S. and C. K. Lee, "Comment on Using The Uniformity Measure for Performance Measure in Image Segmentation", IEEE Trans. Pattern Anal. Machine Intell. Vol. 18, No. 9, pp. 933-935, 1996.

[51] Kapur, J. N., P. K. Sahoo and A. K. Wong, "A New Method for Grey-level Picture Thresholding Using The Entropy of The Histogram", Computer Vision Graphics Image processing, Vol. 29, pp273-285, 1985.

[52] Radhakrishnan, T. K., S. Sundaram and M. Chidambaram, "Non-linear Control of Continuous Bioreactor", Bioprocess Engineering, Vol. 20, pp. 173-178, 1999.

[53] Saha, P., Q. Hu and G. P. Rangaiah, "Multi-input Multi-Output Control of a Continuous Fermenter Using Nonlinear Model Based Controllers", Bioprocess Engineering, Vol. 21, pp. 533-542, 1999.

[54] Wang, F. S., W. C. Lee and L. L. Chang, "On-line State Estimation of Biomass Based on Acid Production in Zymomonas Mobilis Cultures", Bioprocess Engineering, Vol. 18, pp. 329-333, 1998.

[55] Takamatu, T., S. Shiyoya, Y. Okada and M. Kanda, "Profile Control Scheme in Bakers' Yeast Feed-batch Culture", Biotechnology and Biotechnology, Vol. 27, pp. 1675-1686, 1985.

[56] Dochain, D., "Design of Adaptive Linearizing Controllers for Fixed Bed Reactors", Proceedings of the International Control Conference, Baltimore, MD, pp. 335-339, 1994.

[57] Johnson, C.R., K. J. Burnham and D. J. G. James, "Extended Simulation Model for Brewery Fermentation Process", Internatonal Conference on Simulation, 30, pp. 259-262, 1998.

[58] Tan, Y., J. Hu, J. Chang and H. Tan, "Adaptive Integral Backstepping Motion and Experimentation" Industry Applications Conference, 2000. Conference Record of the 2000 IEEE, Vol. 2, pp. 1081-1088, 2000.

[59] Akesson, M., P. Hagander and J. P. Axelsson, "A Pulse Technique for Control of Fed-batch Fermentation", Proceeding of the 1997 IEEE International Conference on Control Applications, Hartford, CT, pp. 139-144, 1997.

[60] Ignatova, M., V. Lubenova and P. Georgieva, "MIMO Adaptive Linearizing Control of Fed-batch Amino Acids Simutaneous Production", Bioprocess Engineering, Vol. 22, pp. 79-84, 2000.

[61] Simeonov, I. S., "Mathematical Modeling and Parameters Estimation of Anaerobic Fermentation Processes", Bioprocess Engineering, Vol. 21, pp. 377-381, 1999.

[62] Konstantinov, K. B., "Monitoring and Control of the Physiological State of Cell Culture", Biotechnology and Biotechnology, Vol. 52, pp. 271-289, 1996.

[63] Jiang, Z. P. and J. B. Pomet, "Backstepping-based Adaptive Controllers for Uncertian Nonhonolomic Systems", Proceedings of the 34th Conference on Decision & Control, New Orleans. LA, pp. 1573-1578, 1995.

[64] Teel, A. R., "Error-based Adaptive nonlinear Control and Regions of Feasibility", International Journal of Adaptive Control and Signal Processing, Vol. 6, pp. 319-327, 1992.

[65] Kanellakopoulos, I., P. V. Kokotovic and A. S. Morse, "Adaptive Nonlinear Control with Incomplete State Information", International Journal of Adaptive Control and Signal Processing, Vol. 6, pp. 369-394, 1992.

[66] Bastin, G., "Adaptive Nonlinear Control of Fed-batch Stirred Tank Reactors", International Journal of Adaptive Control and Signal Processing, Vol. 6, pp. 273-284, 1992.

[67] Queninne, I., B. Dahhau and M. M.Saad, "On Adaptive Control of Fedbatch Fermentation Processes", International Journal of Adaptive Control and Signal Processing, Vol. 6, pp. 521-536, 1992.

[68] Riddler, W. H., and S. Calvard, "Picture Thresholding Using an Iterative Selection Method", IEEE Transactions on System, Man and Cybernetics, Vol . SMC-8, No. 8, pp. 630-632, 1978.

[69] Thrussel, H. J., "Comment on Picture Thresholding Using an Iterative Selection Method", IEEE Transactions on System, Man and Cybernetics, Vol . SMC-9, No. 5, pp. 311, 1979.

[70] Yager, R. R., "On the Measurement of Fuzziness and Negation", Int. Journal of Gen. Sys., Vol. 5, pp. 221-229, 1979.

[71] Kittler, J. and Illingworth, J., "Minimum Error Thresholding", Pattern Recognition, Vol. 19, pp. 41-47, 1986.

[72] Pun, T., "Entropic Thresholding : A New Approch", Comput. Graphics Image Process., Vol. 16, pp. 210-239, 1981.

[73] Chow, C. K. and T. Kaneko, "Automatic boundary detection of the left-ventricle from cineangiograms", Computers and Biomedical Research, Vol. 5, pp. 388-410, 1972.

[74] Kim, H. K., T. T. Nguyen, N. S. Jeong and S. B. Kim, "Nonlinear Adaptive Control of Fermentation Process in Stirred Tank Bioreactor", Proceeding of International Conference on Control, Automation and Systems Engineering, pp. 1939-1942, 2001.

[75] Martinez-Guerra, R., R. Garrido and A. Osorio-Miron, "Parametric and State Estimation by Means of High-Gain Nonlinear Observer: Application to a Bioreactor", Proceeding of the American Control Conference, Alington, VA, pp. 3307-3308, 25-27, 2000.

[76] Busawon, K. and M. Saif, "A State Observer of Nonlinear systems", IEEE Trans. On Automatic Control, Vol. 44, No. 11, pp. 2098-2103, 1999.

[77] Busawon, K. and M. Saif, "A Constant Gain Observer for Nonlinear systems", Proceedings of the American Control Conference, Philadelpia, pp. 2334-2338, 1998.

[78] Busawon, K., M, Farza and H. Hammouri, "Observers' Synthesis for a Class of Nonlinear Systems with Application to State and Parameter Estimation in Bioreactors", Proceedings of the 36th Conference on Decision & Control, San Diego, CA, USA, pp. 5060-5061, 1997.

[79] Farza, H. Hammouri, S. Othman and K. Busawon, "Nonlinear Observer for Parameter Estimation in Bioprocesses", Chemical Engineering Science, Vol. 52, No. 23, pp. 4251-4267, 1997.

[80] Olivera, R., E. C. Ferreira, F. Oliveria and S. Feyo de Azevedo, "A Study on the Convergence of Observer-Based Kinetics Estimators in Stirred Tank Bioreactors", J. Proc. Cont., Vol. 6, No. 6., pp. 367-371, 1996.

[81] Maher, M., B. Dahou and F. Y. Zeng, "Adaptive Filtering and Estimation of Nonlinear Biological System", Journal of Systems, Man and Cybernetics, Vol. 4, pp. 235-240, 1993.

[82] Gauthier J. P., H. Hammouri and S. Othman, "A Simple Observer for Nonlinear Systems Applications to Bioreactor", IEEE Transactions on Automatic Control, Vol. 37, pp. 875-879, 1992.

[83] Tornambe, A., "Use of Asymptotic Observers Having-High-Gains in the State and Parameter Estimation", Proceedings of the 28th Conference on Decision & Control, Tempa, Florida, pp. 1791-1793, 1989.

Publications and Conferences

A. Publications and submissions

[1] Kim, H. K., N. S. Jeong, S. B. Kim and M. S. Lee, "Morphological Feature Extraction of Microorganisms Using Image Processing", Journal of Fisheries Science and Technology, Vol. 4, No. 1, pp. 1-9, Mar., 2001,

[2] Kim, H. K., D. K. Kim, N. S Jeong, M. S. Lee and S. B. Kim, "Reconstruction and Elimination of Optical Microscopic Background Using Surface Fitting Method", Journal of Fisheries Science and Technology, Vol. 4, No. 1, Mar., pp. 10-17, 2001.

[3] Kim, H. K., S. H. Lee, M. S. Lee and S. B. Kim, "A segmentation method for counting Microbial cells in Microscopic image", Transaction on Control, Automation and Systems Engineering, 2001(Submitted).

[4] Kim, D. K., H. K. Kim and S. B. Kim, " Image processing tracking system of multiple Moving Objects Based on Kalman Filter", The Korean Society of Mechanical Engineers, 2001(Submitted).

[5] Kim, H. K., T. T. Nguyen, N. S. Jeong and S. B. Kim, "Nonlinear Adaptive Control of Fermentation Process in Stirred Tank Bioreactor", Transaction on Control, Automation and Systems Engineering, 2001(Submitted).

[6] Kim, H. S., H. K. Kim and S. B. Kim, "Behavior Analysis Method for Fishes in the Water Tank Using Image Processing Technology", Transaction on Control, Automation and Sytems Engineering, 2001(Submitted).

[7] Kim, H. K., T. T. Nguyen and S. B. Kim, "Nonlinear Observer for Applications of Fermentation Processing Stirred Tank Bioreactor", Transaction on Control, Automation and Systems Engineering, 2001 (Submitted).

B. Proceedings and Conferences

[1] Nguyen, V. G., H. K. Kim and S. B. Kim, "Robust pole Assignment in a Specified Disk for Perturbed System", 한국동력기계학회 98 추계 학술대회 논문집, pp. 187-192, Nov. 11, 1998.

[2] 김학경, 예상원, 김상봉, 강지희, 이명숙, "화상처리법을 이용한 질산화세균의 실시간 계측시스템의 개발", 한국정밀기계공학회 1999 년 춘계학술대회논문집, pp. 99-102, May 15, 1999.

[3] Kim, H. K., B. C. Kang, S. H. Lee, S. B. Kim and M. S. Lee, "The measurement of control of nitrifying bacteria by using image processing method", The Japan Society of Mechanical Engineers, Robotics & Mechatronics, 2P1-64-104(2), May, 2000.

[4] 김학경, 이선희, 이명숙, 김상봉, 2000, "암모니아산화세균의 계수를 위한 영상분리기법", ICASE(한국 제어자동화 시스템 공학회, 한국 자동제어학술회의), 560rd-1, Oct. 20, 2000.

[5] Kim, H. K., S. H. Lee, M. S. Lee and S. B. Kim, "A segmentation method for counting ammonia-oxidizing bacteria", Proceedings of The Second Asian Symposium on industrial Automation and Robotics, Bangkok, Thailand, pp. 48-53, May 17, 2001.

[6] Kim, H. K., D. K. Kim, N. S. Jeong, M. S. Lee and S. B. Kim, "Reconstruction and Elimination of Optical Microscopic Background Using Surface Fitting Method", Proceedings of The Second Asian Symposium on industrial Automation and Robotics, Bangkok, Thailand, pp. 176-181, May 18, 2001.

[7] Kim, H. K, N. S. Jeong, M. S. Lee and S. B. Kim, "Chamfer 알고리듬에 기초한 영상분리기법", 2001 대한기계학회 춘계학술대회 논문집 B, pp. 670-675, June 18, 2001.

[8] Kim, H. K, T. T. Nguyen, N. S. Jeong and S. B. Kim, "Nonlinear Adaptive Control of Fermentation Process in Stirred Tank Bioreactor", 2001 International Conference on Control, Automation and Systems Engineering, 1939-1942, Oct. 18, 2001.

미생물의 계수 알고리즘과 생물반응기 시스템의 제어

김 학 경

부경대학교 대학원 메카트로닉스학과

국문요약서

본 논문에서는 생물반응기 시스템의 제어를 위한 이론적 제어계 설계법과 미생물의 계수 알고리즘을 제안하였다. 생물반응기의 제어를 위해서는 반응기 내 미생물의 생장 단계별 균수의 계측이 매우 중요하다. 종래의 미생물 균수 계측 방법으로는 미생물 생육배지를 이용하여 생균수를 측정하는 방법과 현미경을 이용한 직접 계수법이 있다. 생균수 측정법은 오차범위가 작은 반면 24시간 이상 배양하여야 하므로 소요시간이 길다는 단점이 있다. 또한 현미경을 이용한 직접계수법은 현미경을 통해 육안으로 직접 계수함으로서 그 오차범위가 매우 크다고 할 수 있다. 그러나 생물반응기를 실시간적으로 제어를 행할 경우, 계수에 있어 시간적인 한계성을 지닌 육안에 의한 직접계수법을 적용할 수 없으므로, 빠른 시간 내에 정확하게 계수할 수 있는 방법이 요구된다.

이에 본 논문에서는 화상처리법에 기초한 자동계수법을 제안하였다. 화상처리법을 이용할 경우, 그 영상은 보편적으로 많이 사용되고 있는

현미경상에서 CCD 카메라와 전기적 신호처리를 행하는 인테페이스 회로에 의해 얻어지므로, 영상의 밝기는 균일하지 못하며 잡음이 섞여 있게 된다. 이러한 현상은 미생물의 정확한 계수를 어렵게 하는 요인이 된다. 이와 같은 문제점을 제거하기 위해 본 논문에서는 CCD 카메라에 의해 얻어진 초기영상에 대해 여러 가지 잡음과 배경의 불균일한 현상을 제거하는 과정을 거쳐 미생물을 계수하는 알고리즘을 제안했다. 배경의 균일화와 잡음 제거를 위해서는 형상기하학적인 필터와 최소제곱오차법, 2차원 3차 표면적합법과 선형보간법을 이용하였다.

필터링 처리된 영상에 대해 대상으로 하는 미생물의 계수 알고리즘으로써, Otsu의 문턱치 결정법을 수정 보완하여 자동적으로 최적의 문턱치가 결정되도록 제안하였다. 그리고, 기존 watershed 알고리즘의 과도한 영상분리로 인해 그 계수가 정확하지 않던 단점을 보완하기 위한 elongating marker algorithm을 제안하였다. 효모 및 암모니아 산화세균을 대상으로 하여 제안된 계수법을 육안계수법, Otsu법, watershed 계수법 등과의 비교 검토를 통해 그 유효성을 검증하였다.

본 논문에서 제안된 미생물 계수법을 이용하여 생물반응기 내의 배양미생물을 제어하기 위한 기초적인 연구로써, 비선형성을 지닌 프로세서에 적용할 수 있는 비선형 적응제어기 설계법과 시스템의 매개변수와 상태변수를 추정할 수 있는 high gain 관측기의 설계법을 제안하였다. 비선형 적응제어기 설계법은, 반응모델을 기초로 하여 backstepping법에 의해 제안되었다. 목표기질농도의 변화 및 입력기질농도의 변화가 있더라도 희석률을 조정함으로서 목표기질농도에 추종하도록 할 수 있는 제어기 설계법을 보였으며, 시뮬레이션 결과를 통해 그 유효성을 검증하였다. 이 결과로 목표기질농도의 계단변화 및 입력기질농도의 계단변화가 있더라도 희석률을 일정하게 증가시키면 바이오매스 농도를 부드럽게 증가시킬 수 있음을 보였다. 시스템의 매개변수와 상태변수를

추정하는 관측기의 설계법은 Busawan의 관측기를 수정 보완하여 제안하였다. Busawon의 관측기에 유계값을 갖는 시간함수를 고려한 관측기를 제안하였으며, 시뮬레이션을 통해 Busawon 관측기보다 좀더 빨리 그 변수들의 실제값에 수렴할 수 있다는 것을 보였다.

Appendix 1

Otsu's Variance Based Thresholding

In this section, we will show the Otsu's thresholding method that is usually applied to bimodal type histogram in Fig. A1[3-6].

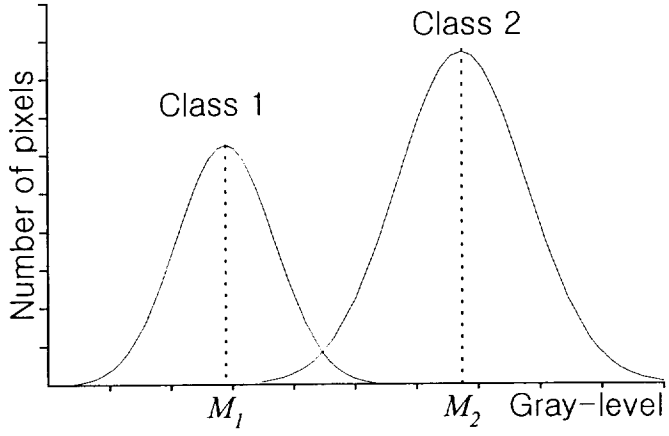

Fig. A1 Statistical meanings of bimodal histogram

The thresholding values are varied according to the positions in the captured image even though the microbial cell type is the same. So, we divide the full image into an appropriate block size with the same pixels and get the thresholding values for each block based on Otsu's method. To adopt the bi-thresholding method, the histogram of an image is converted to a probability distribution.

Let n_i denote the number of pixels at level i. Now if the total number of pixels is denoted by N, then,

$$N = \sum_{i=1}^{L} n_i \tag{A2.1}$$

To facilitate the formulation, the gray-level histogram is normalized and a probability distribution of gray-levels of a given gray level i is obtained:

$$p_i = n_i / N \tag{A2.2}$$

where

$$p_i \geq 0, \ \sum_{i=1}^{L} p_i = 1 \tag{A2.3}$$

Now, let the pixels be thought of as divided into two classes, C_1 and C_2 (background and object or vice versa) which denote respectively the pixels with levels $[1,2,\cdots,k]$ and $[k+1,\cdots,L]$ and k is the required threshold value. The probabilities of occurrence of classes, C_1 and C_2 are given as respectively:

$$\omega_1 = \sum_{i=1}^{k} p_i = \omega_1(k), \quad \omega_2 = \omega_2(k) = \sum_{i=k+1}^{L} p_i = 1 - \omega_1 \tag{A2.4}$$

Similarly, the means of the histogram up to the threshold level $t = k$ in classes, C_1 and C_2 are calculated as respectively:

$$M_1 = \sum_{i=1}^{t=k} i\mathrm{P}(i/C_1) = \sum_{i=1}^{t=k} i\frac{p_i}{\omega_1} = \frac{M(k)}{\omega_1(k)} \tag{A2.5}$$

$$M_2 = \sum_{i=k+1}^{L} i\mathrm{P}(i/C_2) = \sum_{i=k+1}^{L} i\frac{p_i}{\omega_2} = \frac{M_T - M(k)}{1-\omega_1} \tag{A2.6}$$

where

$$M(k) = \sum_{i=1}^{t=k} ip_i, \quad M_T = \sum_{t=1}^{L} ip_i \tag{A2.7}$$

$$\mathrm{P}(i/C_1) = \sum_{i=1}^{k} \frac{p_i}{\omega_1} \text{ and } \mathrm{P}(i/C_2) = \sum_{i=k+1}^{L} \frac{p_i}{\omega_2} \tag{A2.8}$$

which Eq. (A3.8) are the probabilities that gray level i come from the classes, C_1 and C_2.

The between-class variance for the classes, C_1 and C_2 is calculated as follows:

$$\sigma_B^2 = \omega_1(M_1 - M_T)^2 + \omega_2(M_1 - M_T)^2 = \omega_1\omega_2(M_2 - M_1)^2$$
$$= \frac{[M_T\,\omega_1(t) - M(k)]^2}{\omega_1(t)[1 - \omega_1(k)]} \tag{A2.9}$$

Total variance in class $\left(\sigma_T^2\right)$ is as the following equation

$$\sigma_T^2 = \sum_{i=1}^{L} (i - M_T)^2 p_i \tag{A2.10}$$

The optimal thresholding value t is the gray level when the following equation J is maximum.

$$\mathrm{J} = \frac{\sigma_B^2}{\sigma_T^2} \tag{A2.11}$$

Optimal threshold value t is chosen as k to maximize the ratio J of Eq. (A2.11). Since the total variance $\left(\sigma_T^2\right)$, Eq. (A2.10) is constant for a given image histogram, it implies maximizing the between-class variance from Eq. (A2.9).

Bilinear interpolation

Fig. A2 shows a concept of bilinear interpolation method that newly produced pixel is a summation of values multiplying a weighting factor to 4 nearest pixels. Each weighting factor is proportional to distance between pixels.

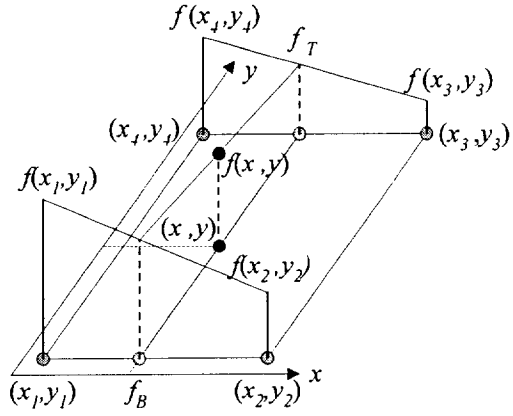

Fig. A2 Bilinear interpolation

The bilinear interpolation is according to the following equations:

$$f(x,y) = f_T - \rho_y(f_B - f_T) \tag{A3.1}$$

where $f(x,y)$ is an approximate function of background.

$$f_B = f(x_1,y_1) - \rho_x\{f(x_2,y_2) - f(x_1,y_1)\} \tag{A3.2}$$

$$f_T = f(x_4, y_4) - \rho_x \{ f(x_3, y_3) - f(x_4, y_4) \} \tag{A3.3}$$

$$\rho_x = \frac{x - x_1}{x_2 - x_1} \tag{A3.4}$$

$$\rho_y = \frac{y - y_1}{y_4 - y_1} \tag{A3.5}$$

And ρ_x, ρ_y are weighting factors for each directions, $f(x, y)$ is a pixel value obtained by interpolation method, (x, y) coordinate of pixel, and (x_1, y_1), (x_2, y_2), (x_3, y_3) and (x_4, y_4) means the four nearest pixels of (x, y).

Appendix 2

Part A

$$\hat{M}\Delta_\lambda(\hat{F} - H\hat{M}^{-1}S_\lambda^{-1}C^TC)\Delta_\lambda^{-1}\hat{M}^{-1}$$

$$= \Delta_\lambda\hat{M}\hat{F}\Delta_\lambda^{-1}\hat{M}^{-1} - \Delta_\lambda\hat{M}H\hat{M}^{-1}S_\lambda^{-1}C^TC\Delta_\lambda^{-1}\hat{M}^{-1}$$

$$= \Delta_\lambda\hat{M}\,\hat{F}\,\hat{M}^{-1}\Delta_\lambda^{-1} - \Delta_\lambda\hat{M}\,H\,\hat{M}^{-1}S_\lambda^{-1}C^TC\Delta_\lambda^{-1}\hat{M}^{-1}$$

$$= \Delta_\lambda HA\,\Delta_\lambda^{-1} - \lambda\Delta_\lambda\hat{M}\,\hat{M}^{-1}H\,\Delta_\lambda{}^{-1}S_1^{-1}\Delta_\lambda{}^{-1}C^TC$$

$$= \lambda A - \lambda\Delta_\lambda H\,\Delta_\lambda{}^{-1}S_1^{-1}\Delta_\lambda{}^{-1}C^TC$$

$$= \lambda(A - H\Delta_\lambda\Delta_\lambda{}^{-1}S_1^{-1}C^TC) = \lambda(A - HS_1^{-1}C^TC)$$

where

$$\hat{M}\hat{F}\hat{M}^{-1} = HA$$

$$C^TC\Delta_\lambda^{-1}\hat{M}^{-1} = C^TC$$

$$S_\lambda{}^{-1} = \lambda\Delta_\lambda{}^{-1}S_1^{-1}\Delta_\lambda{}^{-1}$$

$$\Delta_\lambda HA\Delta_\lambda^{-1} = \lambda\,HA = \lambda\,A$$

Part B

$$2\bar{\varepsilon}^TS_1\dot{\hat{M}}\hat{M}^{-1}\bar{\varepsilon} + 2\lambda\bar{\varepsilon}^TS_1(A - HS_1{}^{-1}C^TC)\bar{\varepsilon}$$

$$= 2\bar{\varepsilon}^TS_1\dot{\hat{M}}\hat{M}^{-1}\bar{\varepsilon} + \lambda\bar{\varepsilon}^T(2S_1A - 2S_1HS_1{}^{-1}C^TC)\bar{\varepsilon}$$

$$= 2\bar{\varepsilon}^TS_1\dot{\hat{M}}\hat{M}^{-1}\bar{\varepsilon} + \lambda\bar{\varepsilon}^T(2S_1A)\bar{\varepsilon} - \lambda\bar{\varepsilon}^T(2S_1HS_1{}^{-1}C^TC)\bar{\varepsilon}$$

$$= 2\bar{\varepsilon}^TS_1\dot{\hat{M}}\hat{M}^{-1}\bar{\varepsilon} + \lambda\bar{\varepsilon}^T(-S_1 + C^TC)\bar{\varepsilon}$$

$$- \lambda \bar{\varepsilon}^T (2S_1 H S_1^{-1} C^T C) \bar{\varepsilon}$$

$$= 2\bar{\varepsilon}^T S_1 \dot{\hat{M}} \hat{M}^{-1} \bar{\varepsilon} + \lambda \bar{\varepsilon}^T (-S_1 + C^T C - 2S_1 H S_1^{-1} C^T C) \bar{\varepsilon}$$

$$= 2\bar{\varepsilon}^T S_1 \dot{\hat{M}} \hat{M}^{-1} \bar{\varepsilon}$$

$$- \lambda \bar{\varepsilon}^T S_1 \bar{\varepsilon} + \lambda \bar{\varepsilon}^T (-C^T C + 2C^T C - 2S_1 H S_1^{-1} C^T C) \bar{\varepsilon}$$

$$= 2\bar{\varepsilon}^T S_1 \hat{M} \hat{M}^{-1} \bar{\varepsilon} - \lambda V$$

$$- \lambda \bar{\varepsilon}^T C^T C \bar{\varepsilon} - 2\lambda \bar{\varepsilon}^T (S_1 H S_1^{-1} - I) C^T C \bar{\varepsilon}$$

$$= 2\bar{\varepsilon}^T S_1 \hat{M} \hat{M}^{-1} \bar{\varepsilon} - \lambda V$$

$$- \lambda \bar{\varepsilon}^T C^T C \bar{\varepsilon} - 2\lambda \bar{\varepsilon}^T S_1 (H - I) S_1^{-1} C^T C \bar{\varepsilon}$$

where

$$\bar{\varepsilon}^T (2S_1 A) \bar{\varepsilon} = \bar{\varepsilon}^T (-S_1 + C^T C) \bar{\varepsilon}$$

Acknowledgments

This thesis could not have been completed without the help and continuous support from professors, colleagues, friends, and family to whom I am most grateful.

First and foremost, I would like to express my sincere gratitude to my supervisor Prof. Sang-Bong Kim, Pukyong National University. He has been a constant source of inspiration and ideas, given me great challenges and been very supportive with all kinds of help. I also would like to express special thanks to Prof. Myung-Suk Lee, the Dept. of Microbiology, Pukyong National University.

I would like to appreciate to my thesis readers, Prof. Gi Sik Byun, Prof. Myung Suk Lee, Prof. Hwan Seong Kim, and Prof. Tan Tien Nguyen for their detailed comments and suggestion during the final phases of the preparation of this thesis.

I would like to appreciate to all advisors: Prof. D. H. Lee, Prof. S. J. Kwon at Pukyong National University, Prof. B. N. Kang, Prof. C. J. Kim and Prof. K. K. Lee, Prof. J. K. Choi at TongMyong College, Prof. I. D. Park, Prof. N. I. Kwak, Prof. I. H. Hwang, Prof. R. B. Park, Prof. D. K. Park, Prof. J. Y. Do, Prof. Y. S. Choi, Prof. S. H. Seo, Prof. S. Y. Lee at Pusan Polytechnic College and Dr. Y. S. Kong for their detailed encouragement and suggestion during my study.

I am also grateful to Dong Kyu Kim for giving me a lot of valuable, interesting and enjoyable discussions, which have contributed substantially to this thesis.

I am also grateful to Jee Hee Kang, Sun Hee Lee, Ji He Kim and other members in Dept. of Microbiology for giving me a lot of valuable, interesting and enjoyable discussions, which have contributed substantially to this thesis.

Thanks are also due to all the members of CIMEC lab for giving me a comfortable and active environment for pursuing my research: Prof. M.S. Shin, Dr. J. W. Lee, H. R. Yoo, Dr. I. K. Kim, C.W. Lee, H .U. Ahn, K. J. Kim, S. M. Kim, N. S. Jeong, S. S. Park, J. O. Kim, B. O. Kam, J. H. Seo, G. Y. Lee, T. K. Yeo, S. K. Jeong, Y. B. Jeon, S. Y. Kim, S. M. Shin, S. J. Park, Y. H. Lee, W. K. Lee, S. W. Kim, H. Y. Kim, J. S. Lim, J. K. Kim, J. N. Kim, J. H. Kim and others. And thanks are also due to all of students Xu Zhe, Trong Hieu Bui and Tan Lam Chung from China and Vietnam for their great encouragement.

I gratefully appreciate the Korea Science and Engineering Foundation(KOSEF) through the Research Center for Ocean Industrial Development (RCOID) at Pukyong National University for their support. I gratefully acknowledge the contributions and suggestions of related persons. I also deliver my thanks to J. J. Kim, Representative at S.J. High Tech and related persons for their support.

I dedicate my sincere thanks and my thesis to my wife and my daughter for their endless encouragement with many cheer and help.

Last but not least, it is my pleasure to thank my parents, my parents-in-law, my brothers, my sisters, my brother-in-law, my sister-in-law, my nephews and my all relatives for their endless encouragement.

Hak-Kyeong Kim